

ANKARA YILDIRIM BEYAZIT UNIVERSITY

GRADUATE SCHOOL OF NATURAL AND APPLIED SCIENCES



**GRAPHENE REINFORCEMENT OF NICKEL-COBALT MATRIX
NANOCOMPOSITES BY DIFFERENT TYPE OF CURRENT
ELECTRODEPOSITION ALLOYS**

M.Sc. Thesis by

Aynur İNAN ÜSTÜN

Department of Materials Engineering

July, 2017

ANKARA

**GRAPHENE REINFORCEMENT OF NICKEL-COBALT
MATRIX NANOCOMPOSITES BY DIFFERENT TYPE
OF CURRENT ELECTRODEPOSITION**

A Thesis Submitted to

The Graduate School of Natural and Applied Sciences of

Ankara Yıldırım Beyazıt University

**In Partial Fulfillment of the Requirements for the Degree of Master of Science
in Materials Engineering, Department of Materials Engineering**

by

Aynur İNAN ÜSTÜN

July, 2017

ANKARA

M.Sc. THESIS EXAMINATION RESULT FORM

We have read the thesis entitled “**GRAPHENE REINFORCEMENT OF NICKEL-COBALT MATRIX NANOCOMPOSITE BY DIFFERENT TYPE OF CURRENT ELECTRODEPOSITION**” completed by **Aynur İNAN ÜSTÜN** under the supervision of **PROF. DR. Hasan OKUYUCU** and we certify that in our opinion it is fully adequate, in scope and in quality, as a thesis for the degree of Master of Science.

Prof. Dr. Hasan OKUYUCU

Supervisor

Prof. Dr. Zafer EVİS

Jury Member

Assist. Prof. Dr. Ramazan KARSLIOĞLU

Jury Member

Prof. Dr. Fatih V. ÇELEBİ

Director

Graduate School of Natural and Applied Sciences

ETHICAL DECLARATION

I hereby declare that, in this thesis which has been prepared in accordance with the Thesis Writing Manual of Graduate School of Natural and Applied Sciences,

- All data, information and documents are obtained in the framework of academic and ethical rules,
- All information, documents and assessments are presented in accordance with scientific ethics and morals,
- All the materials that have been utilized are fully cited and referenced,
- No change has been made on the utilized materials,
- All the works presented are original,

and in any contrary case of above statements, I accept to renounce all my legal rights.

2017, 25 July

Aynur İNAN ÜSTÜN

ACKNOWLEDGMENTS

Firstly, I would like to express my sincere gratitude to my advisor, Prof. Dr. Hasan OKUYUCU, for his tremendous support and motivation during my study.

I also would like to thank Assist. Prof. Ramazan KARSLIOĐLU for his valuable contributions and constructive criticisms during my thesis preparation.

I am grateful to my precious friend Gamze OKYAY for providing me enormous support during my studies and always counting on me.

I must express my profound appreciations to my father for providing me endless support throughout my life.

Finally, I am so grateful to my husband for his endless support and patience. In this achievement, he gave me great support. Thank you.

2017, 25 July

Aynur İNAN ÜSTÜN

GRAPHENE REINFORCEMENT OF NICKEL-COBALT MATRIX NANOCOMPOSITES BY DIFFERENT TYPE OF CURRENT ELECTRODEPOSITION

ABSTRACT

Ni-Co alloys are notable alloys used widely in industry because they have very good wear resistance, high degree of strength and heat conductivity. It is known that third phase addition to alloys improves the properties of them. Graphene has become very popular as a reinforcement material since it has large specific surface and very good electrical, optical, mechanical etc. properties. Electrodeposition is an important coating method because the parameters of the process can be controlled easily during coating process, it doesn't require neither high temperature nor high pressure which result in cost increase and it can be applied complicated shapes. It is known that electrodeposition current type changes coating properties.

In this study copper plates were coated by nickel cobalt alloy and graphene reinforced nickel cobalt metal matrix nanocomposites by electrodeposition coating method. Current types were changed in coating processes. Direct current (DC), pulse current (PC), pulse reverse current (PRC), and ramp current types were applied during electrodeposition. Phase analysis, surface morphology, mechanical and tribological properties were examined. It was observed that properties of coating are enhanced by current type and adding graphene. The best results were obtained when PRC type was used.

Keywords: Ni-Co, graphene, coating, nanocomposite, electrodeposition.

GRAFEN TAKVİYELİ NİKEL-KOBALT MATRİKSİ NANOKOMPOZİTLERİN FARKLI AKIM TÜRÜYLE ELEKTRODEPOZİSYONU

ÖZ

Ni-Co alaşımları üstün aşınma direnci, yüksek mukavemeti, iyi ısı iletkenliğine sahip olmaları sebebiyle sanayide kullanımı oldukça yaygın olan önemli alaşımlardır. Alaşımlara üçüncü faz ilavesinin onların özelliklerini iyileştirdiği bilinmektedir. Grafen çok yüksek yüzey alanı, çok iyi elektrik, optik, mekanik vs. özelliklerinden dolayı katkı malzemesi olarak oldukça popüler olmuştur. Kaplama yöntemlerinden biri olan elektrodepozisyon, üretim esnasında parametrelerinin kolaylıkla kontrol edilebilmesi, fazladan maliyete sebep olan yüksek sıcaklık ve basınç gerektirmemesi ve karmaşık şekillere uygulanabilmesinden dolayı önemli bir kaplama yöntemidir. Elektrodepozisyon akım tipinin kaplama özelliklerini değiştirdiği bilinmektedir.

Bu çalışmada bakır plakalar, elektrodepozisyon kaplama methoduyla nikel kobalt alaşımı ve grafen takviyeli nikel kobalt metal matrisli nano kompozitlerle kaplanmıştır. Kaplamada akım türü değiştirilmiştir. Elektrodepozisyon sırasında Doğru akım (DC), Pulse akım (PC), Pulse-Reverse akım (PRC) ve Rampa akım uygulanmıştır. Faz analizi, yüzey morfolojisi, mekanik özellik ve tribolojik özellikler incelenmiştir. Grafenin ve akım türünün kaplama özelliklerini iyileştirdiği görülmüştür. Akım türünde en iyi sonuçlar PRC'de elde edilmiştir.

Anahtar Kelimeler: Ni-Co, grafen, kaplama, nanokompozit, elektrodepozisyon.

CONTENTS

M.SC. THESIS EXAMINATION RESULT FORM.....	ii
ETHICAL DECLARATION	iii
ACKNOWLEDGMENTS	iv
ABSTRACT.....	v
ÖZ	vi
NOMENCLATURE.....	ix
LIST OF TABLES	xi
LIST OF FIGURES	xii
CHAPTER 1 - INTRODUCTION.....	1
1.1 The Elements.....	2
1.1.1 Nickel	2
1.1.2 Cobalt	4
1.1.3 Copper	6
1.1.4 Graphene	7
1.2 Composite Materials	10
1.2.1 Metal Matrix Composite Materials	12
1.2.2 Nano-Metal Matrix Composite Fabrication Methods	14
1.3 Review of Related Works	24
CHAPTER 2 - EXPERIMENTAL PROCEDURE.....	28
2.1 Preparation of experimental setup and testing.....	28
2.1.1 Preparation of plates.....	28
2.1.2 Preparation of electrolyte bath	29
2.1.3 Electrodeposition processes Ni-Co alloys and Ni-Co-Graphene nanocomposite.....	29
2.2 Characterization of deposited layers.....	32
2.2.1 Scanning electron microscopy analysis.....	32
2.2.2 XRD analysis.....	32
2.2.3 Microhardness measurements (Vickers microhardness tests).....	33
2.2.4 Coating thickness measurements	34
2.2.5 Wear and friction measurements	34

CHAPTER 3 - RESULTS AND DISCUSSION	35
3.1 Structural analysis	35
3.1.1 Microstructural analysis	35
3.1.2 Elemental (EDS) analysis	38
3.1.3 X-Ray diffraction analysis	42
3.1.4 Hardness of coatings	44
3.1.5 Thickness of coatings	46
3.2 Tribological properties	47
3.2.1 Wear and abrasion behavior	47
CHAPTER 4 - CONCLUSION AND FUTURE WORK	54
REFERENCES	56
CURRICULUM VITAE	63

NOMENCLATURE

Abbreviations

A	Atomic weight
Al ₂ O ₃	Aluminum oxide
BaTiO ₃	Barium titanate
BN	Boron nitride
C	Carbon
Co	Cobalt
CoSO ₄	Cobalt sulphate
2-D	Two dimension
e ⁻	Electron
Fe	Iron
F	Faraday constant
H ₃ BO ₃	Boric acid
K	Kelvin
kV	Kilovolt
m	Meter
Ni	Nickel
Nb ₃ Sn	Triniobium tin
n	Valance electron
NiSO ₄	Nickel sulphate
nm	Nano meter
N	Newton
S	Siemens
TP	Terapascal
Q	Net charge passed through the system
V	Volt
WC	Tungsten carbide
Zn	Zinc

Acronyms

A.D.	Anno Domini
B.C.	Before Christ
CNT	Carbon nano tube
CMC	Ceramic matrix composites
DC	Direct current
fcc	Face center cubic
JCPDS	Joint Committee on Powder Diffraction Standards
IMC	Intermetallic compound matrix composites
MEMS	Microelectromechanical system
MMC	Metal matrix composite
pH	Power of Hydrogen
PC	Pulse current
PRC	Pulse reverse current
PC	Pulse current
PRC	Pulse reverse current
SEM	Scanning electron microscope
XRD	X-ray diffractometer

LIST OF TABLES

Table 1.1 Elemental properties of nickel	3
Table 1.2 Elemental properties of cobalt	4
Table 1.3 Elemental properties of copper.....	6
Table 1.4 Dimensional properties of reinforcement materials in composites.....	12
Table 1.5 Possible effects of current type on deposit structures.....	20
Table 2.1 Test parameters of experimental procedure.	30
Table 2.2 Test parameters of all the specimen respectively.....	31



LIST OF FIGURES

Figure 1.1 Application areas of nickel.....	3
Figure 1.2 Application areas of cobalt.....	5
Figure 1.3 Application areas of copper.....	7
Figure 1.4 Allotropes of carbon.....	8
Figure 1.5 Atomic structure of graphene and graphite.....	8
Figure 1.6 Overview of applications of graphene	9
Figure 1.7 CNTs in an epoxy nanocomposite	10
Figure 1.8 Composite types according to reinforcement shape: a) particulate reinforced composite, b) discontinuous fiber reinforced composite, c) continuous fiber reinforced composite	11
Figure 1.9 Schematically representation of electroless plating deposition	15
Figure 1.10 Schematic representation of Cu electrodeposition cell	16
Figure 1.11 Current types: a) DC, b) PC, c) PRC, and d) Ramp current.....	19
Figure 1.12 Process of nanocomposite production by powder metallurgy	21
Figure 1.13 A schematic representation of spray plasma coating method	22
Figure 1.14 A schematic representation of cold spray coating method	23
Figure 1.15 Ni–Co alloy coatings at 50°C for 30 min at 5 A/dm ² current density; (a) DC, (b) PC and (c) PRC methods	26
Figure 1.16 Microhardness of the Ni–Co and Ni–Co/MWCNT.....	26
Figure 2.1 HITACHI Tabletop Microscope TM3030Plus.....	32
Figure 2.2 Picture of XRD instrument	33
Figure 2.3 SHIMADZU HMV-G Vickers microhardness tester.	33
Figure 3.1 SEM surface images of Ni-Co alloys and Ni-Co-Graphene coatings according to current types.	36
Figure 3.2 Weight percentages of elements for Ni-Co coatings	39

Figure 3.3 Weight percentages of elements for Ni-Co-Graphene nanocomposite coatings.....	39
Figure 3.4 EDS Map Sum Spectrum of Ni-Co coating (for Ramp current)	40
Figure 3.5 EDS Map Sum Spectrum of Ni-Co-Graphene coating (for Ramp current)	40
Figure 3.6 EDS dot map analysis of Ni-Co-Graphene coatings produced by ramp current: a) copper, b) nickel, c) carbon.....	41
Figure 3.7 XRD patterns of Ni-Co alloy deposits.....	42
Figure 3.8 XRD patterns of Ni-Co-Graphene nanocomposite deposits	43
Figure 3.9 Crystallite sizes measured by Halder-Wagner method..	44
Figure 3.10 Hardness values for deposits with respect to current types and contents measured by Vickers microhardness test.....	45
Figure 3.11 Thickness of Ni-Co and Ni-Co-Graphene coatings	46
Figure 3.12 Results of wear trace width.....	48
Figure 3.13 Friction coefficient as function of current type in the deposits	49
Figure 3.14 Friction coefficient as function of distance for the Ni-Co alloy deposits produced by pulse current.....	49
Figure 3.15 Friction coefficient as function of distance for the Ni-Co-Graphene alloy deposits produced by pulse current	49
Figure 3.16 Wear track images of Ni-Co alloys and Ni-Co-Graphene composites...51	
Figure 3.17 Ni-Co-Graphene coatings wear trace and EDS dot map analyzes of Ni-Co alloys produced by DC current: a) SEM images, b) map of cobalt, c) map of nickel, d) map of oxygen, e) map of iron, f) map of carbon.	52
Figure 3.18 SEM surface image of wear trace of Ni-Co alloys and Ni-Co-Graphene coatings according to current types	53

CHAPTER 1

INTRODUCTION

Ni-Co alloys have very good wear resistance, high degree of strength, heat conductivity and electrocatalytic activity so these alloys have been extensively used as notable materials in industry. In addition that Ni-Co alloys are used as shape memory alloys and soft magnetic films [2]. Micro-Electro-Mechanical Systems, or MEMS, can be defined as miniaturized mechanical and electro-mechanical elements that are made using the techniques of microfabrication. For MEMS, dimension is critical and their dimensions can be changed from below one micron to several millimeters depending on applications. Properties of films used for MEMS like adhesion, corrosion resistance, thermal stability, strength and magnetic properties must be good so that Ni-Co electrodeposited alloy coatings can extensively be used as recording head materials in computer hard drive industries [3], [4].

There are many studies about Ni-Co alloys in literature which indicated that adding a third material to alloys can improve their properties via producing metal matrix composite. Metal matrix composite is a material that is formed by combining reinforcement material with matrix material. Therefore, the material will have better wear resistance, corrosion properties, friction coefficient, thermal conductivity etc. than alloys [5].

Recently graphene has become very popular among researchers. Graphene, having a 2-D structure, is a basic component of carbon allotropes and composed of six-atom rings in a honeycomb network with one-atom thickness. It has large specific surface area and excellent electrical, optical and mechanical properties. Its Young's modulus, opacity and optical transparency are 1.0 TP (nearly 10 times greater than in steel), 2.3% and 97,9 %, respectively. Due to these superior properties, graphene is used extensively [6], [7].

There are a lot of MMC producing methods one of which is electrodeposition. Electrodeposition has several outstanding properties. It gives the opportunity to

control parameters easily during coating process. Also, it doesn't need high working temperature and pressure conditions and can be applied complicated shapes [2].

Due to these outstanding properties, I aimed to produce graphene added Ni-Co MMC by examining the effect of adding graphene to Ni-Co alloys and current type which can be Direct Current, Pulse Current, Pulse-Reverse Current and Ramp Current. No work on this subject was encountered in literature. Specimens were examined by Scanning Electron Microscope (SEM), Energy Dispersive Spectroscopy (EDS), X-ray Diffraction (XRD), hardness and wear tests.

1.1 The Elements

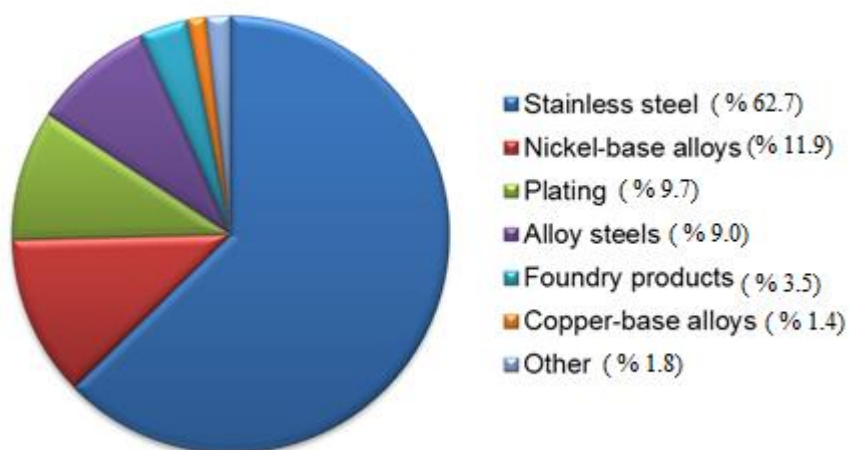
1.1.1 Nickel

Nickel is one of the most abundant elements on Earth. Nickel is not active chemically, its elemental properties are given in Table 1.1. Nickel is a corrosion resistant metal, especially to alkali corrosion. It is ferromagnetic at room temperature. It is a soft metal. It can be tailored at high and low temperatures. It can be welded. For nickel, coldwork and impurity increase its hardness [9]. Nickel is a metal that has been used since the ancient times. Firstly, it was used by ancient men in making knives. A dagger which contains 10.9% nickel, was found at Sumerian city of Ur (about 3100 B.C.). However, Nickel was not known as an element until recently. In 1600s, German miners found the cupronickel but they thought it was a sort of copper. It was identified as an element first by Alex F. Cronstedt in 1751. He heated the cupronickel and it became white and magnetic. He noticed that it was not copper. The New Caledonia mines opened in 1875 and those of Sudbury, Ontario, Canada opened in 1886 are the modern initial mines [8]–[10].

Nickel is one of the most valuable and significant metals for industries. Nowadays, nickel has nearly become the most used element after iron. As the Figure 1.1 shows, it is used in lots of areas such as cast irons, stainless steels, low-alloy steels, special-purpose materials like magnetic alloys and controlled-expansion alloys and it can be used as the base element for many corrosion and heat resistant alloys [9], [10].

Table 1.1 Elemental properties of nickel [8].

Atomic number	28
Atomic weight	58.6934 g/mol
Crystal structure	FCC
Lattice constant	0.35167 nm
Density	8.902 g/cm³
Melting point	1453 °C (2647 °F)
Linear thermal expansion coefficient	0.0000134 K⁻¹
The electrical resistivity	7×10⁻⁸ mΩ
Electrical conductivity	1.4×10⁷ S/m
Curie temperature	358 °C (631°K)
Young modulus	200 GPa
Hardness	195 HV

**Figure 1.1** Application areas of nickel [8].

1.1.2 Cobalt

Cobalt is a metal whose elemental properties are given in Table 1.2. It is ferromagnetic at room temperature so it is generally used for magnetic alloys. It is used together with aluminum and nickel as powerful magnetic materials. In addition, its heat resistance is high, thus it can be used safely where high temperature strength is needed. It has high corrosion resistance but it is affected by precipitation and alloying elements. As the Figure 1.2 shows, cobalt is used in a variety of fields like rechargeable batteries, portable electronic devices, mobile phones, camcorders and computers. Some cobalt alloys can be used as orthopedic implants. Also, cobalt has nonmetallurgical applications such as drying agents for paints, varnishes, inks, batteries and porcelain enamels.

Table 1.2 Elemental properties of cobalt [1].

Atomic number	27
Atomic weight	58,93 g/mol
Crystal structure	HCP (Below 417 °C)
Lattice constant of the fcc form	0.25071, 0.25071, 0.40695 nm
Density	8.85 g/cm³ (similar to nickel)
Melting point	1493 °C
Linear thermal expansion coefficient	0.000013 K⁻¹
The electrical resistivity	6×10⁻⁸ mΩ
Electrical conductivity	1.7×10⁷ S/m
Curie temperature	1131° C (1394 °K)
Young modulus	209 GPa
Hardness	320-330 HV

In ancient times of more than 2000 years ago, cobalt was used as coloring agent (green and blue) for ceramic and glass in Egypt. In China, pottery was produced by using cobalt (A.D. 600 to 900 and A.D. 1350 to 1650). Venetian glass was produced

in the early 15th century with cobalt. First modern cobalt industry was started with the opening of the New Caledonia mines in 1875 [8], [11].

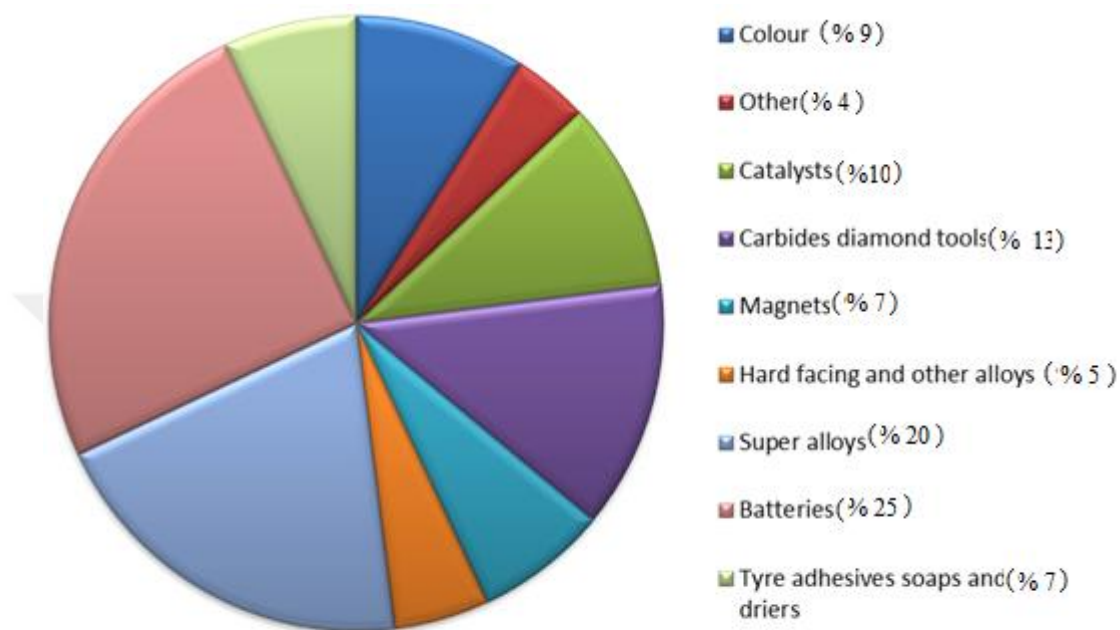


Figure 1.2 Application areas of cobalt [12].

Cobalt is present in nature abundantly. For ores, most of the cobalt can be found in Africa. Moreover, cobalt mines are also present in Canada, Russia, Australia, Finland, and Norway.

1.1.3 Copper

Copper is very important for the civilization. It was used more than 10000 years ago. A lot of historical tools made of copper were found in the Middle East. Some of these tools are made of pure copper in Anatolia. They have been used since approximately 7000 B.C. Bronze Age is started by copper and tin alloys before 3000 B.C. in the Middle East.

Copper has been playing a vital role for the people because of its physical, chemical and aesthetic properties. These properties make it important for domestic, high technology and industrial applications. Copper has high corrosion resistivity, excellent conductivity of heat and electricity and it is malleable and ductile. Copper alloys can be welded by various methods. Its elemental properties are given in Table 1.3.

Table 1.3 Elemental properties of copper [1].

Atomic number	29
Atomic weight	63.546 g/mol
Crystal structure	HCP (Below 417 °C)
Lattice constant of the fcc form	0.36149, 0.36149, 0.36149 nm
Density	8.92 g/cm³
Melting point	1084.62 °C
Linear thermal expansion coefficient	0.0000165 K⁻¹
The electrical resistivity	1.7×10⁻⁸ mΩ
Electrical conductivity	5.9×10⁷ S/m
Magnetic type	Diamagnetic
Young modulus	130 GPa
Hardness	120 HV

Pure copper has high and rapid electrical and heat conductivity so it is extensively used for wires and cables, automobile radiators, heat exchangers and home heating systems. Copper is widely used as an electrical conductor. When it is alloyed with another element, it may have new characteristics. Alloy of copper and tin, that is bronze, is used for carrying potable water systems due to high corrosion resistivity. Its application areas are given in Figure 1.3.

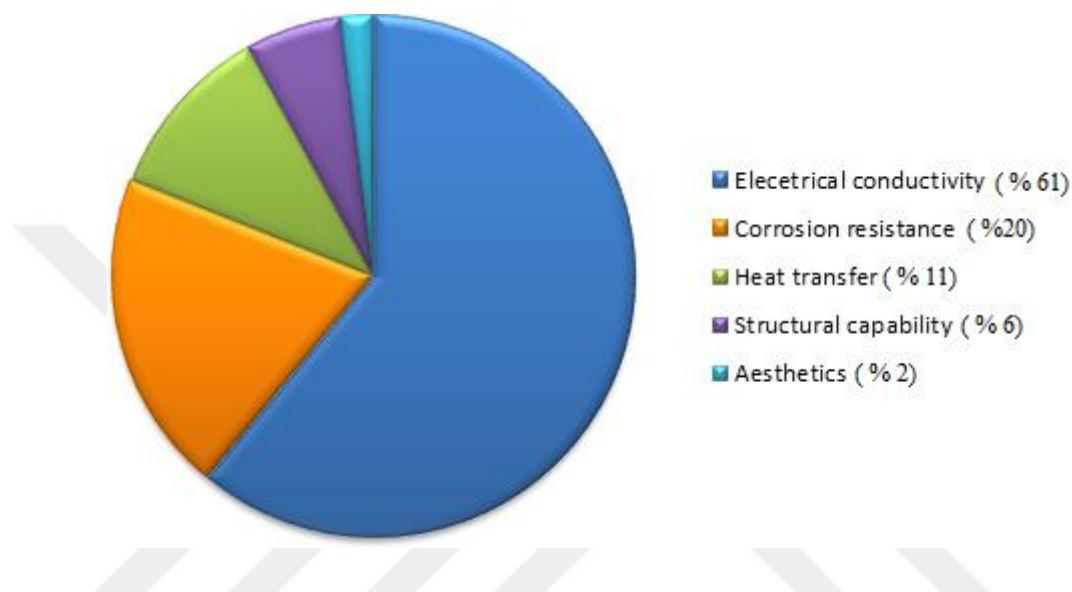


Figure 1.3 Application areas of copper [13].

Copper has very important properties for the green world and humanity. The terms of recycling and reuse of metals have important role in the material selection and acceptance of products. It doesn't degrade or lose its properties in the recycling process. It results in less energy usage, some emissions and waste disposal [13], [14].

1.1.4 Graphene

Graphene is the last found allotrope of carbon. It has two dimensions. Carbon is a metal element. The amount of carbon in the world is very high. It has several allotropes; diamond and graphite have been used since the ancient times. Recently, fullerene and carbon nano tubes (CNTs) were discovered. Thus, zero, one and three dimensions were known. Fullerene, CNT and diamond (or graphite) are zero, one and three dimensional, respectively [15]. The allotropes of graphene are given in Figure 1.4.

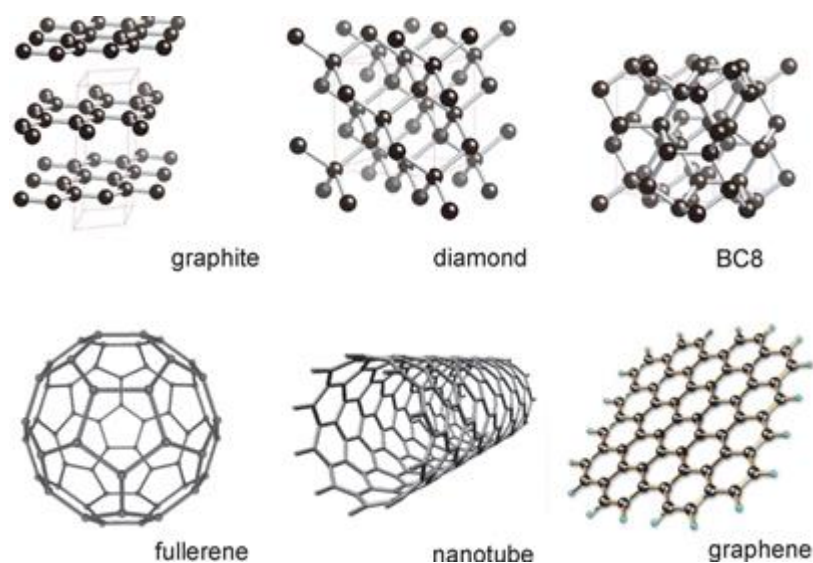


Figure 1.4 Allotropes of carbon [16].

C-C bond length of graphene is nearly 1.42 angstrom. Covalent bonds are strong bonds whereas Van der Waals bonds are weak. It has honeycomb lattice with 2D structure. The structure of graphene is given in Figure 1.5.

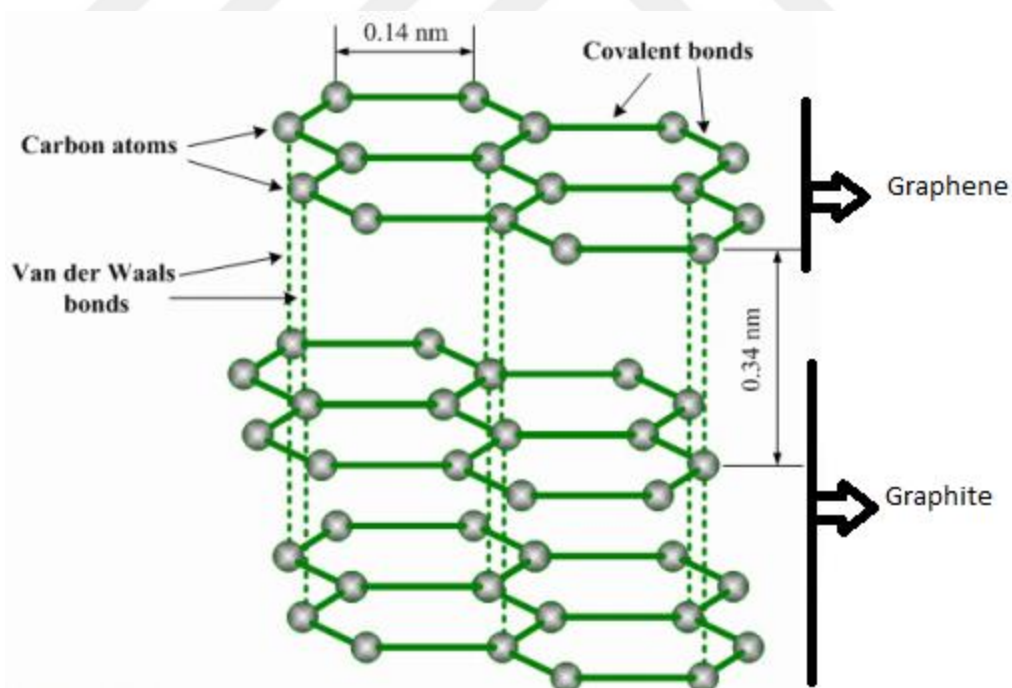


Figure 1.5 Atomic structures of graphene and graphite [17].

Graphene sheet has π (pi) bonds out of plane, that provides a weak interaction, and has σ bonds in plane (covalent bonds) with strong interaction. The π bonds provide the electron conduction to graphene [18].

Its surface area is very high (nearly 2630 m²/g). It has outstanding optical properties (>97.7% transmittance). It has high electron carrier mobility and high Young's modulus (nearly 1000 GPa). Graphene has similar electrical conductivity to copper but its thermal conductivity is five times greater than copper. Its strength is 50 times bigger than that of steel and it has lower density than steel.

Now, graphene is a very famous material which made it possible for its inventors to win the Nobel prize. Andre Geim and his coworkers obtained graphene by an ordinary scotch tape approach using graphite in 2004. Nowadays, there are several production methods for graphene [19].

Due to its superior properties, graphene has many application areas. As the Figure 1.6 shows, it is used in electronic devices, gas sensors, magnetoresistance, transparent conducting electrodes, nanoelectromechanical systems, membranes, supercapacitors, lithium ion batteries, fuel cells, solar cells, composites etc. [20].

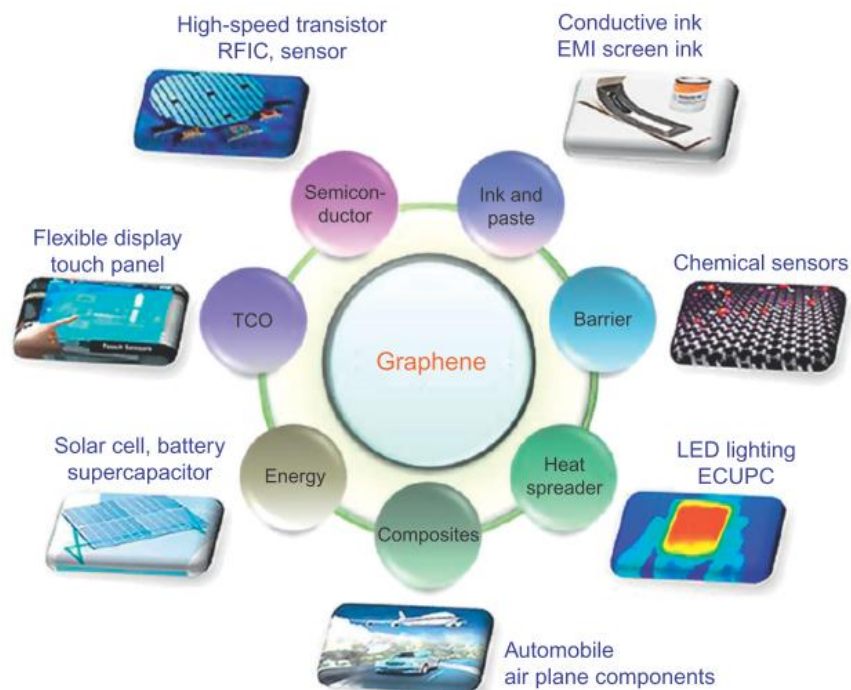


Figure 1.6 Overview of applications of graphene [19].

1.2 Composite Materials

Composite materials have more than one phase by artificial combination of different materials so that composite materials can have improved properties. This combination doesn't occur with natural means like reactions, phase transformations etc. Moreover, this combination is not atomic or molecular level. Each material retains its own properties but this is not the case when considering alloys. Alloys have completely different properties from the elements that form them. Composite materials can be produced for various properties. The components of materials can be chosen by considering their distribution, morphologies, degrees of crystallinity and crystallographic textures. The composites can be arranged in any desired manner. Thus, they have a lot of application areas such as automobile, aerospace, biomedical, electronics, energy, construction, and other industries.

In order to understand and visualize composite materials, a lightweight structural composite material which is composed of discontinuous carbon nanotubes embedded in a polymer matrix is shown as an example in Figure 1.7 [21].

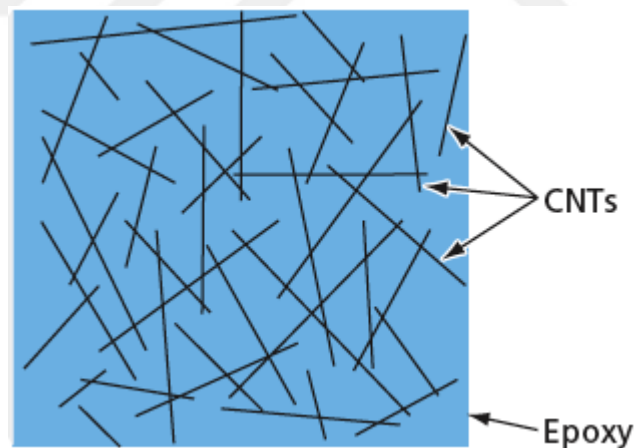


Figure 1.7 CNTs in an epoxy nanocomposite [16].

By adding CNTs, the material gains low density that is lower than aluminum, high strength that is as strong as high-strength steel, high stiffness that is stiffer than titanium, high creep resistance, high fatigue resistance, low friction coefficient and good wear resistance.

Generally, composites are classified in six groups according to matrix materials:

- metal matrix composites (MMC),
- polymer matrix composites,
- ceramic matrix composites (CMC),
- glass matrix composites,
- intermetallic compound matrix composites (IMC),
- carbon fiber reinforced carbon (CC composites).

Another classification method is according to reinforcement shape. There are three types:

- particulate reinforced composite (see Figure 1.8-a),
- discontinuous fiber reinforced composite (see Figure 1.8-b),
- continuous fiber reinforced composite (see Figure 1.8-c) [22], [23].

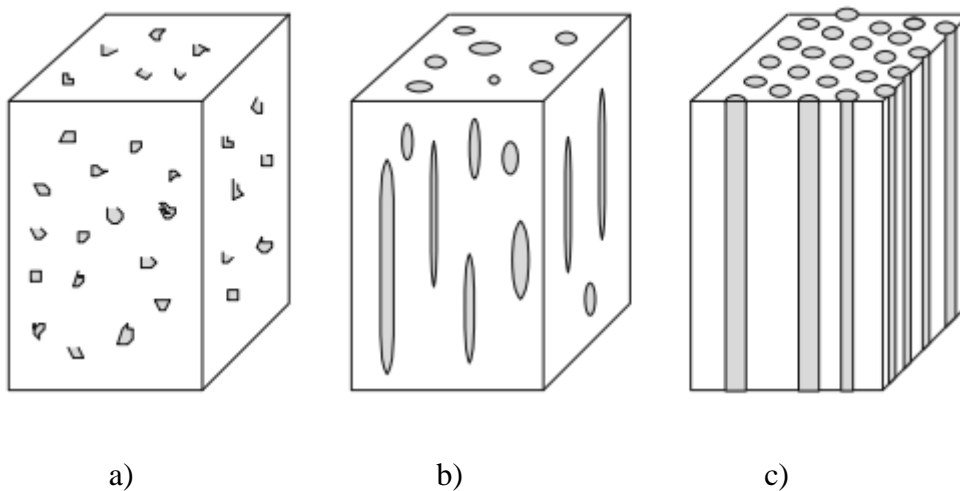


Figure 1.8 Composite types according to reinforcement shape: a) particulate reinforced composite, b) discontinuous fiber reinforced composite, c) continuous fiber reinforced composite [24].

Several properties of reinforcement materials are given in Table 1.4.

Table 1.4 Dimensional properties of reinforcement materials in composites [23].

Reinforcement type	Ratio of Width- Length	Size, μm	Examples
Particulate	1-4	25	SiC, Al ₂ O ₃ , BN, WC
Short fiber	10-10000	1-5	C, SiC, Al ₂ O ₃
Continuous fiber	>1000	3-150	SiC, Al ₂ O ₃ , Nb ₃ Sn

1.2.1 Metal Matrix Composite Materials

Metal matrix composites (MMC) are generally formed by combining two materials which are matrix and reinforcement materials. Matrix is generally metal or its alloys and reinforcement can be generally intermetallic compound, oxide, carbide or nitride. MMC has generally good performance in corrosive ambient and at high temperature.

In addition, they have high elastic modulus, high strength, low density, high electrical and thermal conductivity [23]. Good wear resistance can be obtained through MMC by ceramic reinforcement materials. MMCs can be strengthened by plastic deformation [22].

MMC fabrication methods are:

- powder techniques;
- deposition;
- casting;
- diffusion bonding;
- in situ reinforcement;
- deformation processed [23].

Nanocomposites are the composites at least one of whose components has nanometer scale structure. Size is around 10^{-9} m. When the constituents of materials are nano size, they can obtain superior properties. Nano size constituents provide good mechanical, chemical, optical, magnetic and electrical properties. Especially high hardness and good wear resistance can be obtained by nanocomposites. For example, CNT reinforcement into the matrix could result in good electrical and thermal conductivity [21], [25].

In order to reduce fuel consumption and emissions in transportation, light alloys have been used in structural components. High performance and low weight structural materials are very important in a wide range of industrial applications. For example, aluminum and magnesium alloys have good mechanical properties, castability and high thermal conductivity but their mechanical properties decrease relatively at low temperatures, hence addition of hard reinforcement materials in it can improve these properties. MMCs have superior properties than conventional composites but they have some limitations such as low ductility and toughness. To minimize these bad effects, reinforcement size was decreased in MMCs [26].

Nanocomposites have obtained great attention. In 1986 there were 2 articles and in 2004 there were 1690 articles according to Google Scholar. In nanocomposites, interfaces are very important to increase and decrease general properties of materials. In nanostructure, interfaces constitute the smaller volume fraction of the matrix material. This case cannot be obtained in conventional composites. Interfaces of conventional composites cause to weak regions. When nano size reinforcement materials are added to ceramics, properties are relatively enhanced. For example, functional ceramics such as ferroelectric, piezoelectric, varistor ceramics materials can be enhanced by nanocomposites technology. Adding a small quantity of ceramic or metallic nanoparticle into BaTiO_3 can increase its strength, hardness and toughness. These properties are very important for safety electric devices operating in severe environmental conditions. Addition of soft materials into hard ceramics generally decreases its mechanical properties; however, soft materials added to some ceramics can improve their mechanical properties in nanocomposites. For instance, addition of hexagonal boron nitride to silicon nitride ceramic can enhance their

fracture strength from room temperature to 1500 °C [27]. By adding 10% nanoceramic reinforcement material into epoxy, wear resistance can be doubled and scratch resistance can be increased to 50% [28].

Nanocomposites can be fabricated simply with low cost. They can be fabricated by electrodeposition, powder metallurgy, spray coating, mechanical alloying and casting. Wetting between matrix and reinforcement materials is an important problem which must be enhanced. For nanocomposites to have good properties, reinforcement materials need to be well dispersed [23].

1.2.2 Nano-Metal Matrix Composite Fabrication Methods

1.2.2.1 Electroless Plating

Electroless plating, chemical process, is a method of plating that not use external power source. Thus, this fabrication method is simpler than electroplating. Electrons to be used for reducing metal ions are obtained from baths [29].

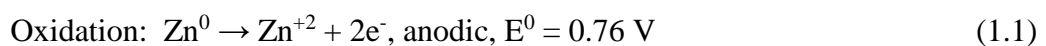
In an aqueous solution of a metal salt, chemical deposition of a metal occurs by electrochemical mechanism. Solution reacts with chemical species and oxidation and reduction reactions occur between these species by electron transfer (see Figure 1.9). Oxidation, anodic process, means that substance losses electron and reduction, cathodic reaction, means that substance gains electrons [30].

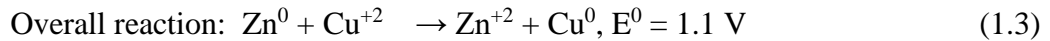
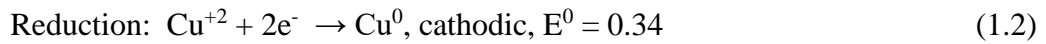
There are generally two methods for electroless deposition:

- Deposition by ion or charge exchange
- Metal deposition by reduction substance from bath [23].

Example of deposition by ion exchange; zinc is immersed in a copper sulphate solution; zinc dissolve due to it is less noble metal. Then copper atoms deposit on the zinc plate and occur deposition. This displacement occurs until all zinc surface coating by copper. By this method, deposition layer is only a few microns.

For example, immersion deposition reaction (see Eq. (1.1), Eq. (1.2), Eq. (1.3)):





For deposition, reactants must be diffused to the surface and then adsorbed. Chemical reaction occurs on the surface. Residual products are desorbed and diffused away from the surface.

Not to consume substrate and to obtain a thick deposition, electroless plating is used. To make the deposition, there must be a source of metal ions, a reducing agent, suitable mixing agents and stabilizers [30].

For example, reactions of metal deposition by reduction substance (see Eq. (1.4), Eq. (1.5), Eq. (1.6)) are: [30].

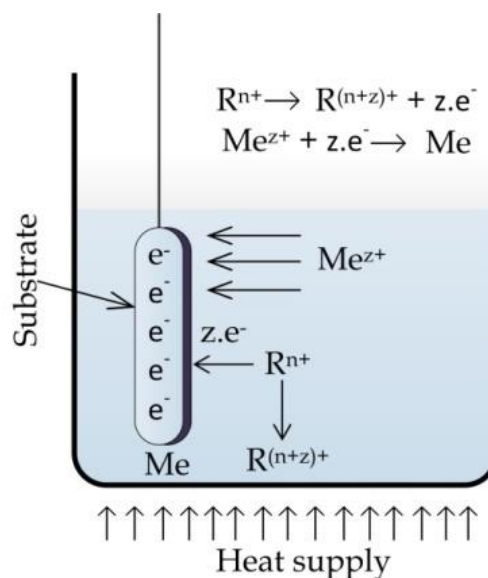
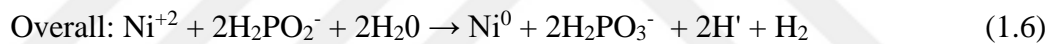
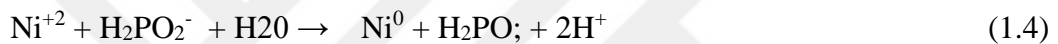


Figure 1.9 Schematically representation of electroless plating deposition [31].

Deposits with less porous and good uniformity can be obtained by electroless depositions. Electroplating cannot provide these properties because of the differences in current density concentration. Non-conductive materials like ceramics and plastics can be coated by electroless fabrication method. Nevertheless, this method has some disadvantages; its bath is more complicated than electrolytic deposition bath. In electroless deposition, new materials must be added when they are consumed [31],[32].

1.2.2.2 Electrodeposition

Electrodeposition is a process of a film growth onto a base material by electrochemical reduction of metal ions from an electrolyte (see Figure 1.10). Electrolyte is an ionic conductor. It combines suitable solvent and deposition materials. Solvent is usually water but it can be an organic compound. This process occurs in a vessel which contains electrolyte, anode and cathode electrodes and a power supply. They make possible the current flow from cathode to anode. Required electrons are obtained by power supply. In electrodeposition, the material to be coated is connected to negative terminal of the power supply. Thus, metal ions are reduced on the cathode to metal atoms and deposition is achieved [28], [29].

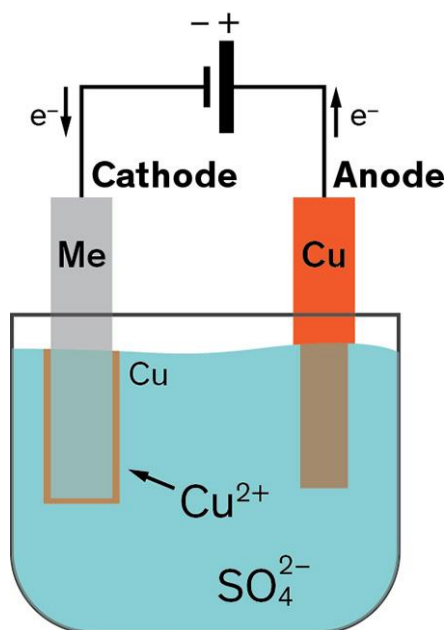


Figure 1.10 Schematically representation of Cu electrodeposition cell [33].

General reaction for metal formation is given by Eq. 1.7.



L may be ion, radical or molecule, such as H₂O, CN⁻ or SO₄²⁻. It tightly bonds to the metal ion and they together form complex species. These complex species take role in the charge transfer process.

“n” is the net quantity of electrons transferred during the process. It must be positive. “z” is the electric charge of the electroactive species in electron units. It can be positive, negative or zero.

Deposition process occurs according to Faraday’s law which is given in Eq. 1.8.

$$m = QA/nF \quad (1.8)$$

“m” is the deposited metal mass in gram. “A” is the atomic weight of the metal. “F” is the Faraday constant ($F = 96485 \text{ C mol}^{-1}$). “n” is the valance electron of metal. “Q” is the net charge passes through the system, current multiply with time.

Electrodeposition occurs from simple solution. They may be salt or other soluble compounds containing the metal in the form of anion, cation or complex.

For good electrodeposition, some additives need to be used. For the solution to have electrical conductivity, inorganic acid or alkali can be added. By this way, the conductivity can be increased whereas the voltage applied can be decreased. In addition, acid and alkali materials can be used as pH regulator. In order to obtain completely homogenous bath in terms of acidity, buffer agents can be added into the bath. Some of the additives can reduce the electrode surface energy so they can inhibit the attachment of hydrogen bubbles to surface. These bubbles lead to undesirable pitting that is macroscopic point defects.

Electrodeposition process is affected by several parameters: temperature, pH, current density, current type and substrate. Temperature is a very important parameter. Temperature is usually kept between 15 – 70 °C. Increasing temperature increases solubility and electric conductivity. However, excessive temperature promotes the

additive adsorption and this may result in more coarse-grained deposits. Substrate can influence nucleation of the deposition. The surface treatment enhances the deposition quality. Moreover, concentration can influence the electrical conductivity. Dilute solution can cause more fine-grained coatings and lower deposition rate. Stirring causes ion to transport and decreases diffusion layer. pH level changes hydrogen evolution and hydroxides precipitation [34].

In electrodeposition, current is an important factor for plating quality. There are several current types like direct current, pulse current, pulse-reverse current and ramp current and their schematic representations are given in Figure 1.11. Qu and et. al. found that in nickel electrodeposition, hardness of specimen produced by PC method was higher than those produced by DC method. Tao et. al. produced copper electrodeposition plating and achieved higher hardness and wear resistance with PC method than DC method. As compared to DC type, PC method is more flexible as it is easier to control the parameters. Microstructure, constituents and their combination of plating layer can be controlled with on and off time of PC type [23]. Chang et. al. examined the Pulse-Reverse current since DC and PC methods are not adequate. In pulse-reverse process, when reverse current was applied, reverse transition occurred opposite to current direction. Reverse transition increases electrochemical polarization of cathode, hence nucleation energy decreases, nucleation rate increases and more compact structure and more smooth surface is obtained [35]. In Table 1.5, deposition events are given during on time, off time and negative on time.

Electrodeposition is a highly important fabrication method. This technology is not very expensive and a lot of available materials can be used as a coating material [29]. Recently electrodeposition methods have been widely used in microelectronic industry. Electrodeposition fabrication method can be safely used for materials with good corrosion resistance, good wear resistance and good thermal and magnetic properties. Electrodeposition provides thin or thick layer deposition.

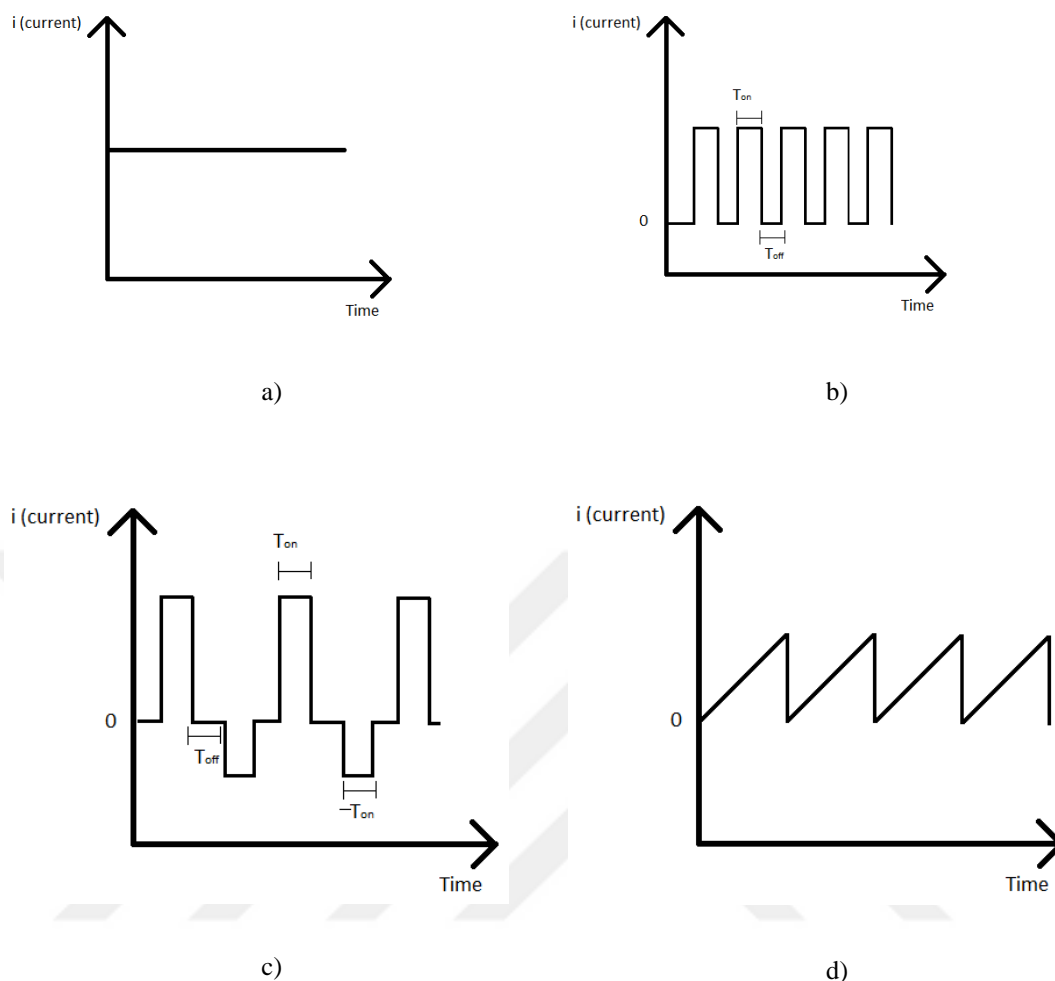


Figure 1.11 Current types: a) DC, b) PC, c) PRC, and d) Ramp current [36], [37].

Many significant and valuable materials can be produced by the help of electrodeposition. Fe-alloys fabricated by electrodeposition materials get significant importance for data collection and detection. IBM increased recording density from 10 times per decade to 100 times per decade by the electrodeposited permalloy [4].

Table 1.5 Possible effects of current type on deposit structures [38].

Time Interval	Conditions that differ from DC plating	Phenomena affected
On-time	Double layer charging Overvoltage Concentration profile near the electrode Adsorption (ions, additives, hydrogen)	Nucleation rate Growth mechanism Electrode reaction mechanism Codeposition rate Additive reaction
Off-time	Double layer discharge Potential relaxation Desorption (ions, additives, hydrogen)	Surface diffusion Surface recrystallization Corrosion, displacement reactions Passivation Hydrogen diffusion
Pulse-reverse time	Anodic potential Sign change of double layer charge Concentration profile near electrode Desorption / adsorption (additives, ions)	(selective) Metal dissolution Hydrogen reoxidation Additive oxidation Passivation

1.2.2.3 Powder metallurgy

This method is applied at lower temperatures and there is no liquid phase. Thus, microstructure can easily be controlled. Also, it provides dimensional stability. Because of these advantages, it is widely selected [39]. As the Figure 1.12 shows, steps in powder metallurgy can be given as follows:

- Powder production
- Compaction
- Sintering
- Secondary and other finishing operations [40].

When nanocomposites are produced, several problems can be encountered. Agglomeration and nonhomogeneous dispersion can be occurred. In literature, in order to eliminate these problems, a high energy ball milling technique has been employed [39].

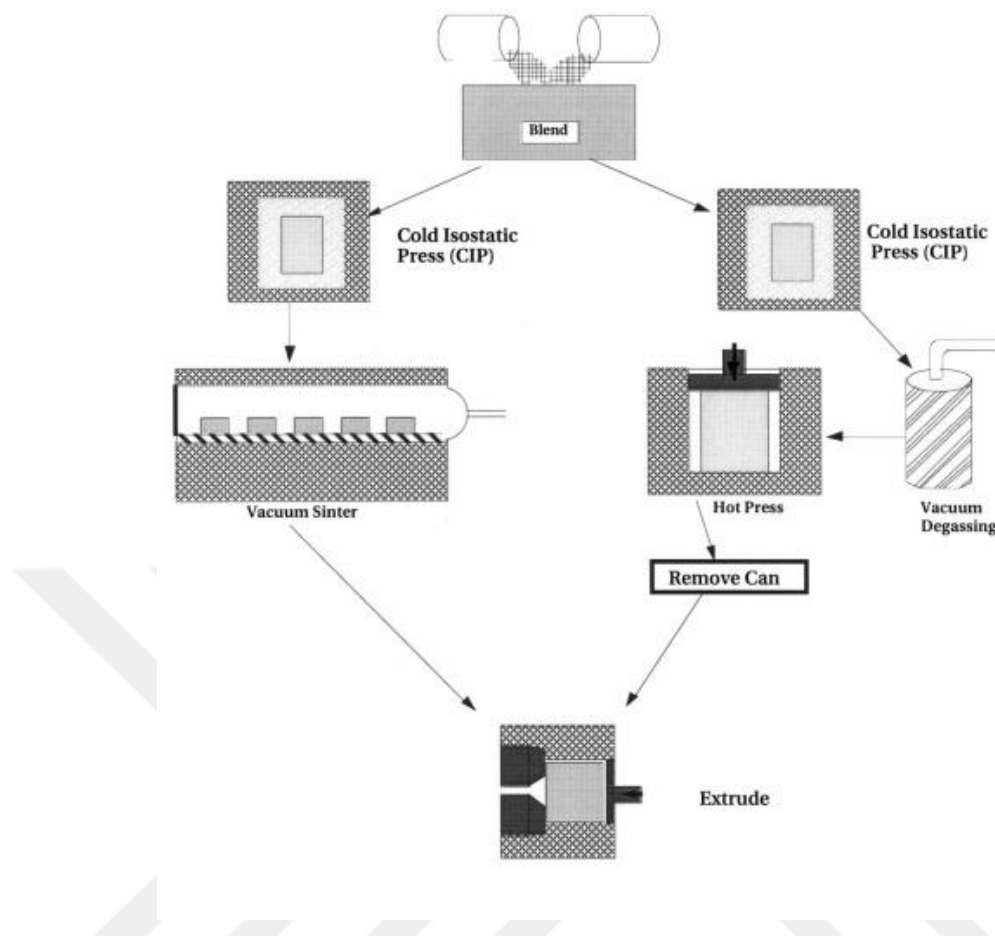


Figure 1.12 Process of nanocomposite production by powder metallurgy [39].

1.2.2.4 Spray plasma coating

As the Figure 1.13 shows, spray plasma coating is a liquid phase technique. Molten metal is sprayed and coated onto the substrate. Plasma which is the fourth state of matter is condensed gas form. This phase contains free electrons and positive ions whose quantities are equal to each other. By spray plasma technique, all materials can be melted. They can be applied in inert atmosphere. However, this method has some several disadvantages; porous materials may be produced and densification is needed which means extra production cost [21], [41].

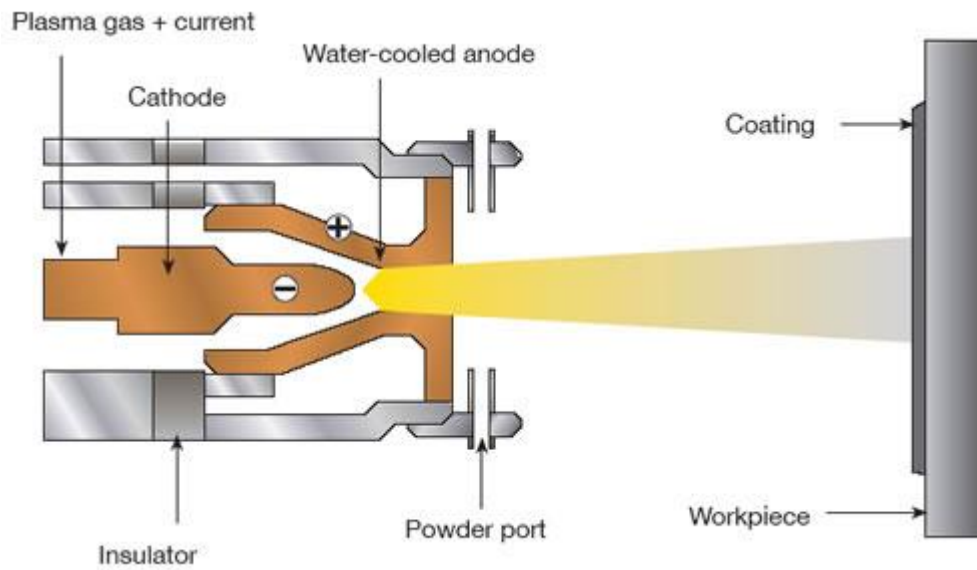


Figure 1.13 A schematic representation of spray plasma coating method [42].

1.2.2.5 Cold spray coating

Cold spray coating means that temperature of sprayed materials is lower than their melting temperature. Its principle is high velocity of coating materials, nearly 300-1200 m/s. It is appropriate for nanocrystalline coating. For the other methods like spray plasma coating, oxidation, phase transition or chemical decomposition may be occurred. There may be several reasons one of which is high temperature for these undesirable results [43]. As compared with conventional coating, low temperature is the advantage for this method. By this method, coarse grained copper deposits can be produced and their electrical conductivity will be close to bulk copper [44]. The production stages are given schematically in Figure 1.14.

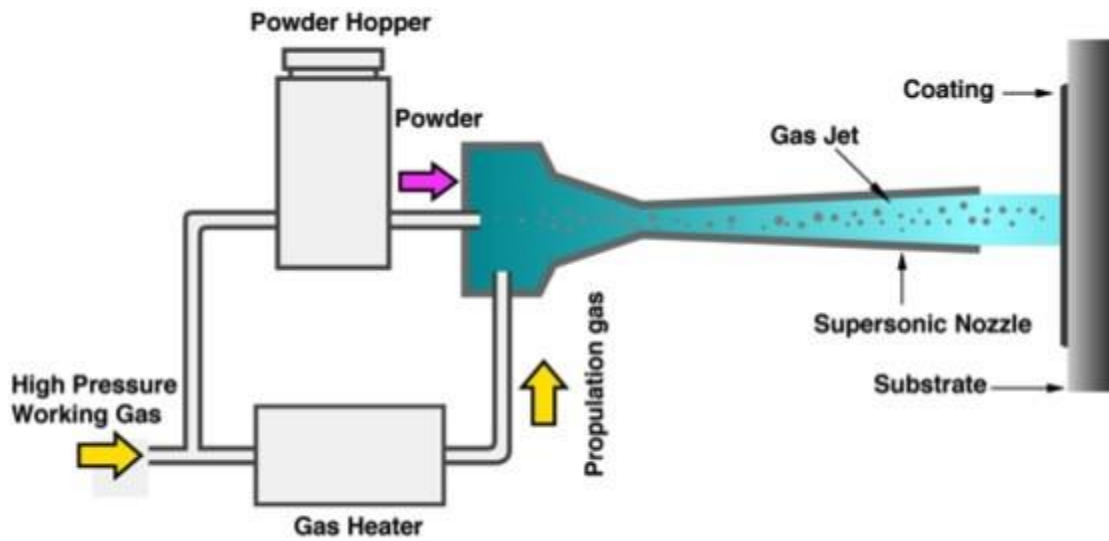


Figure 1.14 A schematic representation of cold spray coating method [45].

1.2.2.6 Molecular level mixing process

In this process, reinforcement materials are mixed in matrix materials by molecular level. In order to produce carbon nanotubes, conventional methods were not enough and new methods were required. In literature, some CNT nanocomposites were produced by several methods. However, their properties were not enough. For example, CNT/alumina nanocomposites were produced by blending dispersed and spark plasma sintering method was applied. For this nanocomposite, fracture toughness increased whereas hardness decreased with the increase in amount of CNT. Such results led new methods to be found. Molecular level mixing process carries out the steps below:

- producing reinforcement materials and mixing them in liquid homogenously,
- mixing and seeding reinforcements and matrix phase
- drying at 200-300°C
- sintering [25].

1.3 Review of Related Works

Ni-Co alloys can be widely used in industry because of their important properties. For example, they have high-strength, good wear resistance, heat conductivity and corrosion resistivity. These alloys are used since they have good magnetic properties. They can be used as a shape memory alloys. Electrodeposition method is useful for Ni-Co alloys because it need not high temperature and pressure [2],[8]. Micro-Electro-Mechanical Systems (MEMS) have thickness from nanometer to a few millimeters. This technology is used in recording head material in hard drive industries. Due to superior magnetic properties, Ni-Co alloys and composites are extensively used for MEMS. make increase Corrosion resistivity, mechanical strength, abrasion resistance and chemical and biocompabilities are increased by metal-matrix composite coatings, hence they have superior properties to alloys [3]. Adding nano-size ceramic particles can enhance tribological and wear properties of materials. Ni-Co alloys have better wear, hardness and corrosion properties than Ni coatings. It has been reported that adding nano size reinforcement materials to alloys enhances their properties further. Electrodeposition with direct current is known as easiest and the most convenient method. However, new methods like pulse current and pulse-reverse current have been examined in recent years. They have been compared with direct current and they may enhance microstructure, mechanic and corrosion properties [46].

It is known that electrodeposition parameters change the deposition properties. One of these parameters is current type. Some of known current types are direct current, pulse current, pulse-reverse current and ramp current. In direct current, current density is constant during deposition process. For pulse current, current is applied cathodic direction during Time_{on} and then current become zero during Time_{off} periodically. During the electrodeposition process, a time-dependent negatively charged layer forms around the cathode surface and prevents the cation ions from reaching the cathode surface. By pulse current, this layer can dissolve to a certain level. The difference of pulse reverse current from other current types is the fact that current is applied in negative direction so negatively charged layer is decomposed when the current applied. Thus, smaller grain size can be obtained by these methods.

During the off time, desorption of the impurities increases the recrystallization. Relatively low residual stress can be obtained by pulse reverse technique to produce pure Ni - Co alloys and this technique increases hardness. By this technique, there is no need to use the additives. In addition, with pulse-reverse technique void-free nickel coatings can be obtained. It is declared in literature that SiC content increase in Ni - SiC composites by PRC method [37].

Hu et al. [47] worked on Ni – SiC composite coatings by electrodeposition method. They investigated current effects on the deposition properties. They used ramp current that are ramp up and ramp down. In their studies, SiC particles are dispersed homogenously with ramp current. Under low current density, agglomerations occur. They reported that zero current inhibits grain growth so new nucleus can occur.

Shi et al. [3] have reported that addition of CNT to Ni-Co alloys increases mechanical and tribological properties of composite coatings as compared to Ni-Co alloys due to the fact that CNT decreases the grain size. Meanwhile, CNT decreases the friction and wear.

Karslıoğlu et al. [46] examined the effects of current type and addition of MWCNT on Ni-Co alloys. They declared that addition of CNT to Ni-Co alloys changes the wear mechanism and increases surface roughness. It may be caused by agglomeration of MWCNT. When compared according to current types, hardness level and MWCNT content change from high to low with PRC, PC and DC, respectively. The crystallographic grain growth orientation changes and it effects hardness (see Figure 1.16). The results show that DC type cause bigger grain size (see Figure 1.15). XRD results show that addition of MWCNT changes morphology from polyhedral structure to spherical structure and decreases grain size. The coating thickness decreases by PRC method because of the fact that this method increases MWCNT content and it inhibits the grain growth rate so thinner coatings are obtained. They say that the wear mechanism changes with reinforcement material. Wear trace of Ni-Co alloys is on all surface but it occurs on the ridge in nanocomposites. Furthermore, elemental analysis shows that alloys exhibit oxidizing on all the surface but nanocomposites only exhibit on protrusions.

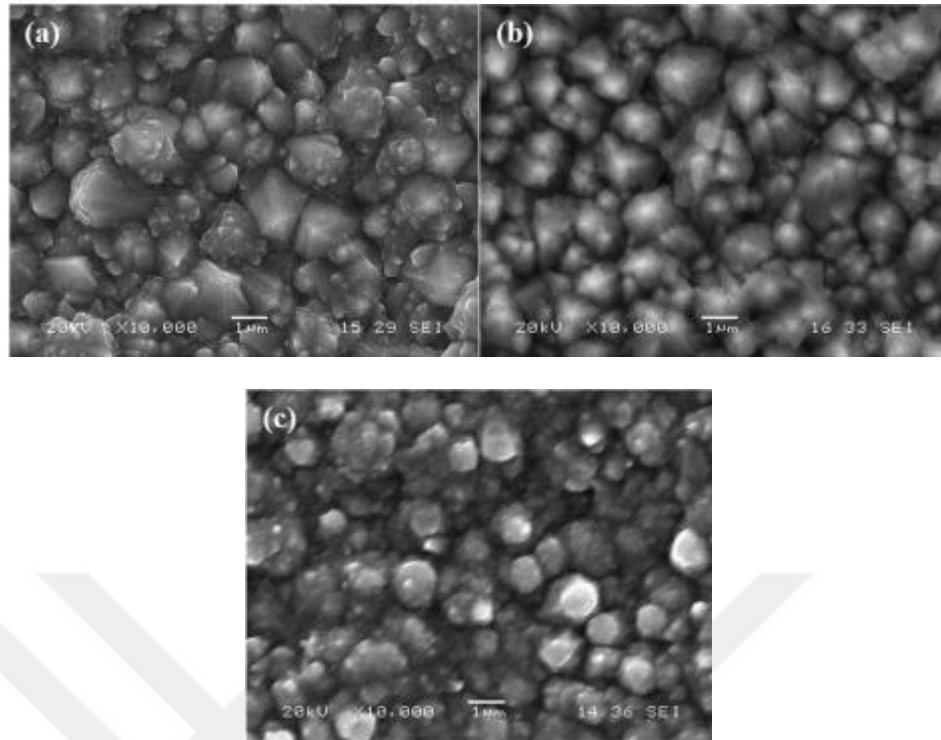


Figure 1.15 Ni–Co alloy coatings at 50°C for 30 min at 5 A/dm² current density; a) DC, b) PC and c) PRC methods [46].

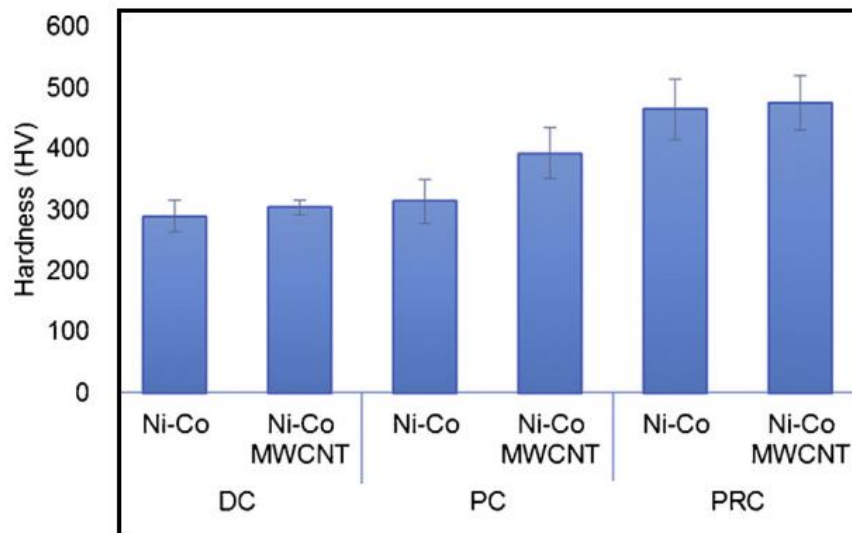


Figure 1.16 Microhardness of the Ni–Co and Ni–Co/MWCNT [46].

Srivastava et al.[48] worked microhardness and corrosion resistance of Ni-Co alloys. They declared that when cobalt content increases up to 50 wt.%, hardness increases, however if content continues to increase, hardness decreases since the crystallographic morphology changes from spherical crystal to polyhedral crystal.

When cobalt content reaches up to 80 wt.%, crystallographic morphology changes to acicular shape. Their study shows that 80% Ni – 20% Co alloy exhibits better corrosion resistance than plain nickel or cobalt coating and then other mixing percentages. This is correlated with FCC structure of alloy. Their results show that corrosion currents of mild steel, cobalt coating, nickel coating, Ni-20% Co and Ni-50% Co are 2.994, 2.602, 0.527, 0.455 and 0.894 $\mu\text{A}/\text{cm}^2$, respectively.



CHAPTER 2

EXPERIMENTAL PROCEDURE

All the experimental processes were conducted at Ankara Yıldırım Beyazıt University. For electrodeposition process, Watt type bath was used. Process temperature is usually kept about 40-65°C for Watt type bath. Current density and pH are 2-10 A/dm² and 4.7-5.1, respectively. Electroplating device, BARAKUDA current source located at laboratories of Ankara Yıldırım Beyazıt University, was used as power supply. It can provide direct current, pulse current, pulse-reverse current and ramp current. Coatings were carried out in 100 ml glass beaker with speed controlled magnetic stirrer (ISOTEX) in fume hood. As a cathode material, copper plates with high purity were used with the dimensions of 20x30x2 mm as width, length and thickness, respectively. As anode material, nickel was used with the dimensions of 30x40x3 mm as width, length and thickness, respectively. Coating baths contained high purity nickel sulphate (NiSO₄.6H₂O), cobalt sulphate (CoSO₄.7H₂O), boric acid (H₃BO₃) and distilled water. For composite coatings, graphene was used. It had 3 nm x 1,5 µm dimensions. An ultrasonic mixer was used to prevent agglomeration of the graphene in the bath.

In this study, effects of the addition of graphene to nickel-cobalt coating and the different current types were investigated on microstructure, hardness and wear resistance properties.

2.1 Preparation of experimental setup and testing

2.1.1 Preparation of plates

In this study, copper plates were used as cathode with the dimensions of 20x30x2 mm as width, length and thickness, respectively. The substrates must be clean so that the coatings can be well stick on to the substrate and a homogeneous coating is obtained. Cu plates were grinded with grinding paper that had 60, 180, 400 and 600 grid size. Before the coating, plates were dipped into HCl for 10 seconds and then cleaned with distilled water.

2.1.2 Preparation of electrolyte bath

Two types of bath which are for Ni-Co alloys and Ni-Co-Graphene nanocomposites were prepared. Used bath was a Watt type bath and electrolyte bath was prepared in 100 ml glass beaker. The coatings contained 25 g of nickel sulphate ($\text{NiSO}_4 \cdot 6\text{H}_2\text{O}$), 5 g of cobalt sulphate ($\text{CoSO}_4 \cdot 7\text{H}_2\text{O}$), 4 g of boric acid (H_3BO_3), 0.1 g of graphene and 100 ml of distilled water. Baths were stirred for 10 minutes with magnetic stirrer. For graphene reinforcement coating, ultrasonic stirrer was used to prevent agglomeration of graphene for 30 minutes. Then coating systems were prepared in the fume hood. Bath temperature was about 50 ± 5 °C. Four specimens were coated. Direct current, pulse current, pulse-reverse current and ramp current were applied. Deposition time was 30 minutes. Test parameters are shown in Table 2.1.

2.1.3 Electrodeposition processes Ni-Co alloys and Ni-Co-Graphene nanocomposite

Because of literature researches, it was decided to use Watt type bath that contains nickel sulphate ($\text{NiSO}_4 \cdot 6\text{H}_2\text{O}$), cobalt sulphate ($\text{CoSO}_4 \cdot 7\text{H}_2\text{O}$) and boric acid (H_3BO_3). Nickel sulphate is nickel source, cobalt sulphate is cobalt source and boric acid regulates pH of the bath. For graphene reinforced Ni-Co nanocomposites, 1g/L graphene was added. pH is an important quality of coating for electrodeposition and it must be constant at 4. Bath temperature was constant at about 50 ± 5 °C. Magnetic stirrer also functions as heat supply and has heat probe. Thus, bath temperature could be kept constant at 50 ± 5 °C.

DC, PC, PRC, and ramp current type were used at 7 A/dm^2 in processes. Effects of these current types were examined on the coatings. Four specimens were produced as Ni-Co alloys. First specimen was produced by DC method and the others were produced by PC, PRC and Ramp current methods. Four specimens of Graphene reinforced Ni-Co nanocomposites were produced by same methods. Current types are shown schematically in Figure 1.11.

Table 2.1 Test parameters of experimental procedure.

	Ni-Co alloy coatings	Graphene reinforcement Ni-Co nanocomposite coatings	
Bath and coating parameters	NiSO ₄ ·6H ₂ O (Nickel source)	250 g/L	250 g/L
	CoSO ₄ ·7H ₂ O (Cobalt source)	250 g/L	250 g/L
	H ₃ BO ₃ (pH regulator)	250 g/L	250 g/L
	Graphene (reinforcement material)	-	1 g/L
	Current density	Average 7A/dm ²	Average 7A/dm ²
	Current type	DC, PC, PRC, Ramp	DC, PC, PRC, Ramp
	pH	4	4
Temperature	50±5 °C	50±5°C	
Magnetic stirring	Before deposition: 10 minutes During deposition: 30 Minutes	Before deposition: 10 minutes During deposition: 30 Minutes	
Ultrasonic stirring	-	After magnetic stirring: 30 minutes	
Cathode	Nickel	Copper	

Graphene has nanosize dimensions and agglomeration occurs very easily, hence graphene reinforced electrolytic bath were stirred through ultrasonic homogenizer for 30 minutes, different from Ni-Co alloys. Ultrasonic homogenizer provides good homogenous mixing. Ultrasonic homogenizer uses sound waves with high frequency components to disrupt material into smaller particles [49]. Thus, agglomeration can be prevented in a more efficient way than magnetic stirrer.

In Table 2.2, bath parameters are given for Ni-Co alloys and graphene reinforced Ni-Co nanocomposites.

Table 2.2 Test parameters of all the specimen respectively.

Specimen No:	Current	Graphene	NiSO ₄ .6H ₂ O/ CoSO ₄ .7H ₂ O/ H ₃ BO ₃ (g/l)	T _{on} / T _{off} / -T _{on} (ms)
1	7 A/dm ² Current density _{max} : 420 mA/6cm ²	-	25/5/4	∞/0/0
2	7 A/dm ² Current density _{max} : 840 mA/6cm ²	-	25/5/4	10/10/0
3	7 A/dm ² Current density _{max} : 910 mA/6cm ²	-	25/5/4	10/10/10
4	7 A/dm ² Current density _{max} : 840 mA/6cm ²	-	25/5/4	10/1/0
5	7 A/dm ² Current density _{max} : 420 mA/6cm ²	1 g/l	25/5/4	∞/0/0
6	7 A/dm ² Current density _{max} : 840 mA/6cm ²	1 g/l	25/5/4	10/10/0
7	7 A/dm ² Current density _{max} : 910 mA/6cm ²	1 g/l	25/5/4	10/10/10
8	7 A/dm ² Current density _{max} : 840 mA/6cm ²	1 g/l	25/5/4	10/1/0

2.2 Characterization of deposited layers

2.2.1 Scanning electron microscopy analysis

For characterization process, images of scanning electron microscopy were examined with HITACHI Tabletop Microscope TM3030Plus (see Figure 2.1) and results were compared with literature. How the grain structure changed under different conditions was examined. With the same device, EDS (electron dispersive spectroscopy) analysis was conducted and the elemental ratio was examined.



Figure 2.1 HITACHI Tabletop Microscope TM3030Plus [50].

2.2.2 XRD analysis

In this study, Cu $K\alpha$ X-ray beam source was employed during examinations which operated at 40 kV. The analysis was performed at $2^\circ/\text{min}$ scan rate between 40° to 100° 2θ angles by using X-ray diffractometer (Rigaku Miniflex 600, see Figure 2.2). The phase identification of the selected alloys was performed by using a diffraction analysis program (PDXL). Crystallite sizes were found by this analysis according to Halder-Wagner methods.



Figure 2.2 Picture of XRD instrument.

2.2.3 Microhardness measurements (Vickers microhardness tests)

Microscale mechanical properties were examined with SHIMADZU HMV-G Vickers microhardness tester in Material Engineering Department of Ankara Yıldırım Beyazıt University. Microhardness measurements were conducted under 9.807 N load and holding time of 10 seconds by diamond pyramid indenter. Figure 2.3 shows SHIMADZU HMV-G Vickers microhardness tester. At least five measurements were taken from each specimen.

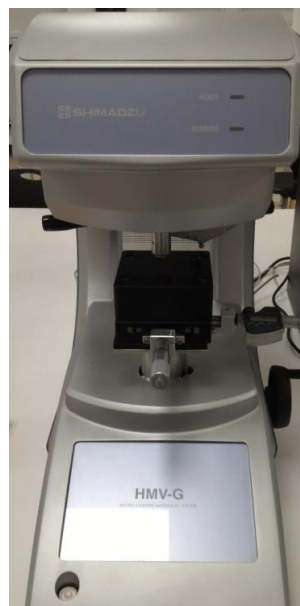


Figure 2.3 SHIMADZU HMV-G Vickers microhardness tester.

The Vickers microhardness equation (Eq. 2.1) can be written as follows:

$$\text{Vickers Microhardness} = \frac{2F \sin \frac{136^\circ}{2}}{\left(\frac{d_1 + d_2}{2}\right)^2} \quad (2.1)$$

F: Test load

d_1, d_2 : lengths of diagonal

2.2.4 Coating thickness measurements

Coating thicknesses were measured by electromagnetic measurement probe. Before the measurements, device was reset and the measurements were conducted from five different areas. Finally, their averages were calculated.

2.2.5 Wear and friction measurements

Wear and friction tests were conducted by speed of 25 mm/s, 2 N loading, 12 mm trace width and 500 m distance reciprocal movement. Friction coefficients were recorded by the software program. Wear trace width was measured by optical microscope.

CHAPTER 3

RESULTS AND DISCUSSION

3.1 Structural analysis

3.1.1 Microstructural analysis

Similar studies about electrodeposition of Ni-Co alloys and reinforced Ni-Co nanocomposites were examined in literature and optimum parameters were aimed to adopt for this study [3], [51]–[53]. The effects of current type and the difference between reinforced and nonreinforced structures on the properties of Ni-Co alloys and Ni-Co-Graphene nanocomposites are examined. These structures are generally used for magnetic purposes, hence pure copper plate was chosen as a substrate. According to examinations in literature, Co content changes the coating parameters in Ni-Co alloys and Ni-Co composites. Optimum cobalt content was examined to be found from literature and it is decided that nickel and cobalt quantity should be 250g/l and 50g/l, respectively. Whereas $\text{NiCl}_2 \cdot 6\text{H}_2\text{O}$ is added to electrolytic bath [35] in some studies, this is not the case for some other studies [46], [54]. In some cases, addition of NiCl_2 may cause pitting on the deposition surface, for this reason it was decided not to add NiCl_2 in this study. H_3BO_3 is used as a pH regulator substance for electrodeposition so it was used during the processes and pH value was kept on 4 during the coating processes. Finally, electrolytic bath was made up of 25 g of nickel sulphate ($\text{NiSO}_4 \cdot 6\text{H}_2\text{O}$), 5 g of cobalt sulphate ($\text{CoSO}_4 \cdot 7\text{H}_2\text{O}$), 4 g of boric acid (H_3BO_3) and 100 ml of distilled water.

It is understood that current type is an important electrodeposition parameter and it can change deposition properties as noticed in SEM images given in Figure 3.1. When compared the Ni-Co alloy specimens according to current type, DC type electrodeposition has bigger grain size than PC type and PC has bigger grain size than PRC. Grain size of the specimens produced by ramp current is in between that of PC and PRC type. Grain size has an effect on the hardness value of specimen. Smaller grain size has higher hardness value than the bigger grain size [46]. In this

thesis, the hardness results and XRD results verify our SEM images. When the alloys and composites are to be compared, composites have smaller grain size and a more rough surface. This may be due to agglomeration or additional deposition mechanism [46].

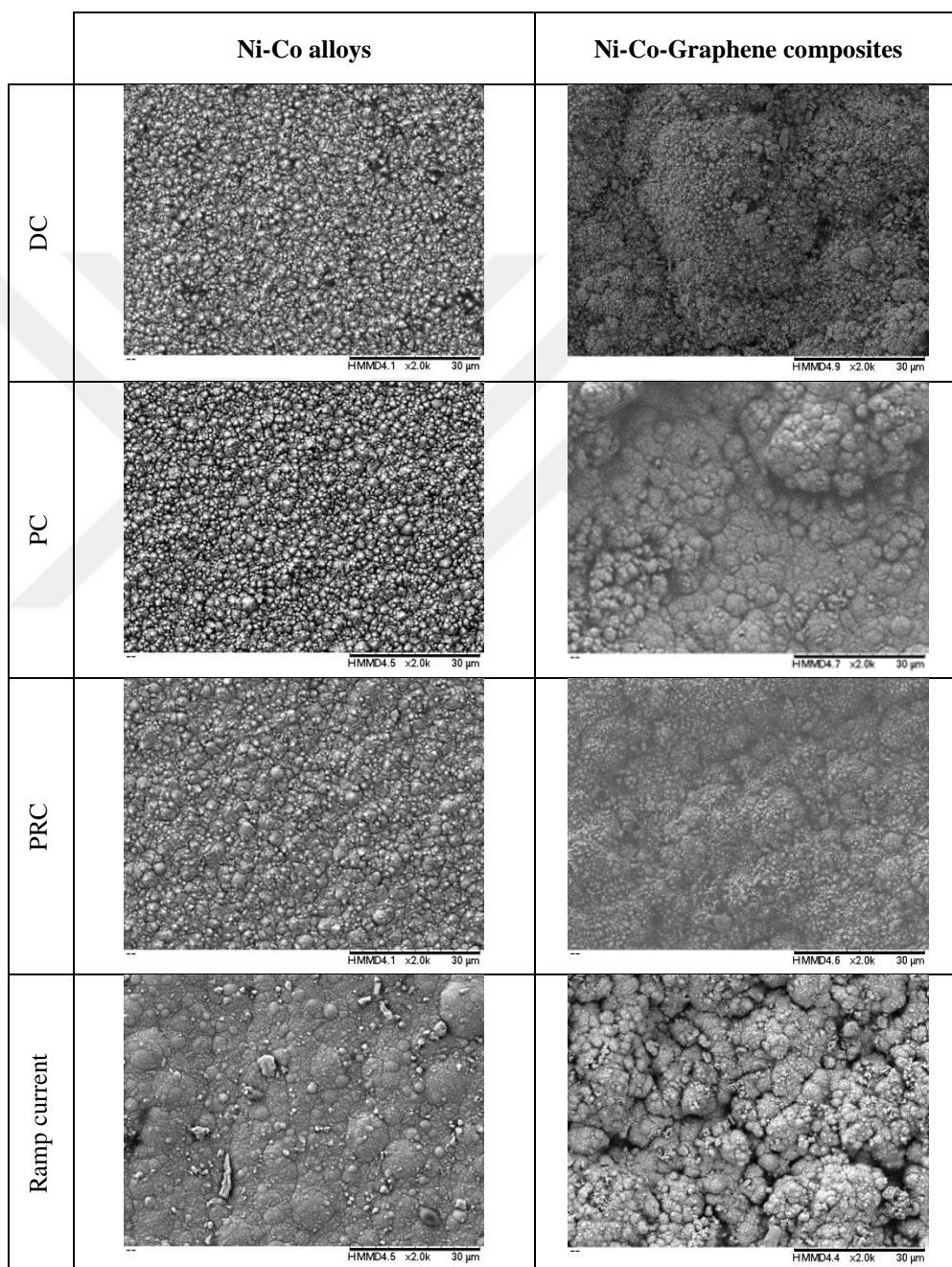


Figure 3.1 SEM surface images of Ni-Co alloys and Ni-Co-Graphene coatings according to current types.

Hu et al. [47] have worked on the effects of ramp current type on the Ni - SiC composites and revealed that ramp current increase homogenous dispersion of SiC reinforcement in Ni matrix material according to SEM images.

Landolt et al. [37] declares that pulse current type positively affects the microstructure, composition, mass transport and improves current distribution.

According to several studies, addition of nano-size second phase like Ni-Al₂O₃ nanocomposites as a reinforcement material enhances the properties of coatings because reinforcement material inhibits matrix material grain growth. Thus, grain size can decrease down to 30 nm by DC current. Steinbach et al. [55] reported in their studies that lower agglomerated degree can be obtained by PR current type than DC current type and they concluded that deposition materials can be selected according to particle size with PR current type. They reported that nanosize particles are embedded more efficient than large particles. During the T_{off} of PC current type, current is not supplied which inhibits grain growth and desired particle size can be obtained. Chang et al. [35] report that Al₂O₃ reinforced Ni-Co nanocomposites produced by PRC have smoother surface than those produced by PC method. They declare that specimen produced by PRC method ensures finer grain size and more density. Impurities are removed from the surface during the -T_{on}, hence more compact surface can be obtained. Steinbach et al. think as similar to Chang et al. that Al₂O₃ locates on the interfaces and causes to inhibit the grain growth. PRC technique increases electrochemical polarization of cathode so nucleation energy decreases. Thus, finer grain size can be obtained.

Ranjith et al. [56] examined the effects of current type and addition of TiO₂ on the Ni-Co alloys and composites. They declare that addition of TiO₂ increases hardness of the Ni-Co alloys. TiO₂ works as a barrier for the grain boundaries so grain sizes get smaller and finer grain is obtained by adding reinforcement material. When the current types are compared, smoother surface is obtained by pulse reverse current type than pulse current type. Grain sizes with pulse reverse current are smaller than the ones with pulse current. However, when composites are compared, pulse reverse current lets TiO₂ disperse along the grain boundary and it inhibits grain size to increase. Furthermore, they declare that changing the current direction decreases

nucleation energy and increases number of nuclei for pulse reverse current. Thus, finer grain size is obtained by pulse reverse current.

3.1.2 Elemental (EDS) analysis

The elements and their ratios in the alloys and composites were investigated by Energy Dispersive Spectrometer. Similarly, this technique is used in some studies [57].

The elements and their percentages in Ni-Co alloy and Ni-Co-Graphene composite are given in Figure 3.2 and Figure 3.3, respectively. It is seen that current type affects the elemental ratio of deposits. Co ratio is the highest in specimen produced by DC type electrodeposition. Elemental ratio values are similar to each other for DC and PC types. However, cobalt ratio is smaller than nickel in PRC case, different from other current types. For ramp current, cobalt ratio is greater than the one for PRC but smaller than those of other current types. In contrast, except for the ramp current, nickel rate increases with DC, PC and PRC types, respectively. Nickel ratio is in between the ratios of PC and PRC. Ni-Co-Graphene composites have similar elemental ratios as compared to Ni-Co alloys. The highest nickel content is in the PRC deposits whereas the smallest quantity is in the DC types. When considering the graphene, its ratio increases with DC, PC, PRC and ramp current, respectively. The ratio of the graphene has the highest value for ramp current whereas the smallest ratio for graphene is obtained for DC current. EDS analysis was conducted after graphene had been added to Ni-Co alloys. EDS Map Sum Spectrums of Ni-Co coating and Ni-Co-Graphene coating produced by ramp current are given in Figure 3.4 and Figure 3.5. Moreover, EDS map results are given in Figure 3.6. The elements are homogeneously distributed in deposits. Carbon in the coatings comes from the addition of graphene.

Wang et al. [51] reported that cobalt content in alloys is always higher than cobalt content in electrolytic bath. They thought that cobalt is a less noble element than nickel and it is preferentially deposited. It is widely known that pH value changes near electrodes, therefore metal hydroxyl forms and competitive adsorption occurs.

Some studies declare that reinforcement material content increase in the deposition by pulse-reverse current type nearly by six times [37].

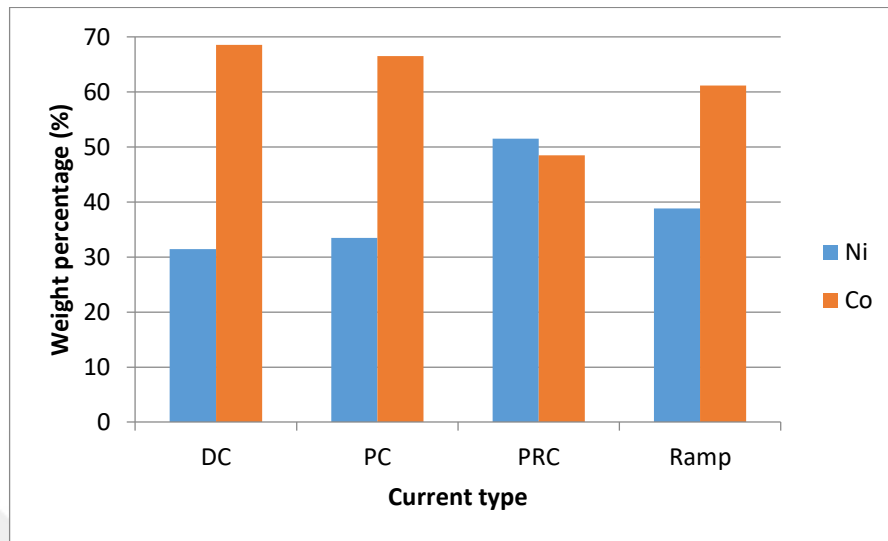


Figure 3.2 Weight percentages of elements for Ni-Co coatings.

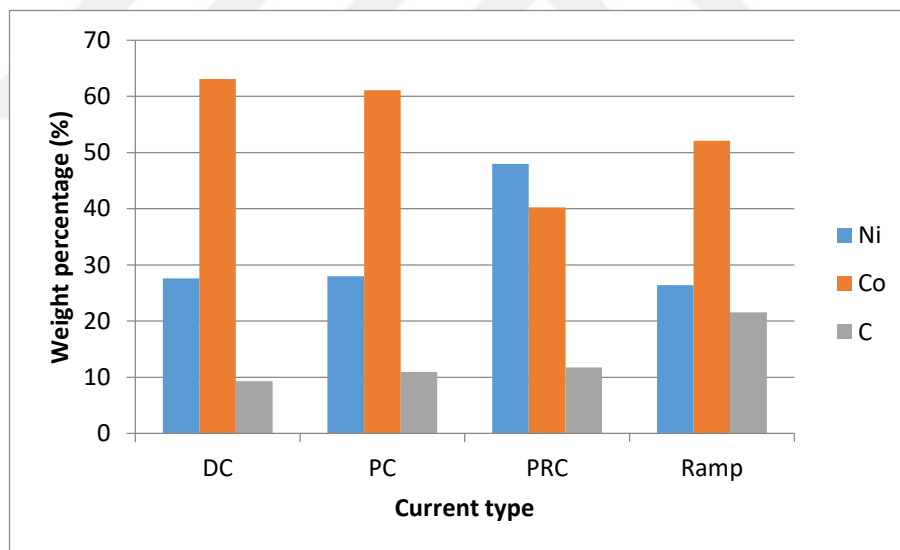


Figure 3.3 Weight percentages of elements for Ni-Co-Graphene nanocomposite coatings.

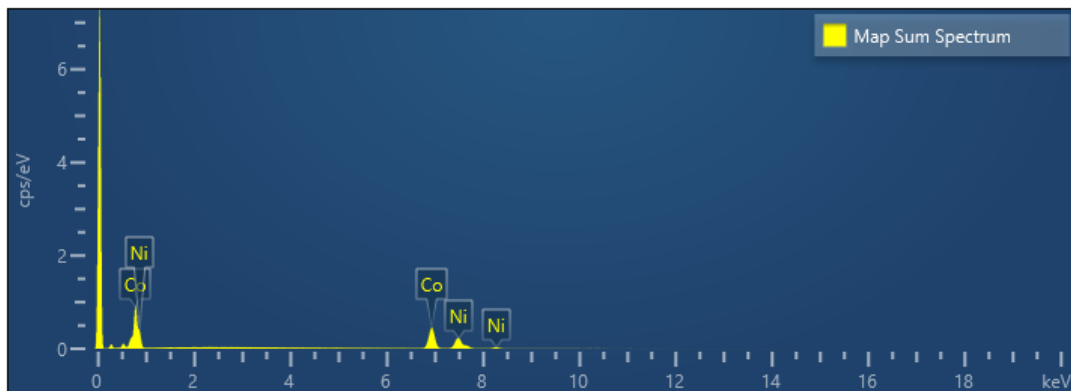


Figure 3.4 EDS Map Sum Spectrum of Ni-Co coating (for Ramp current).

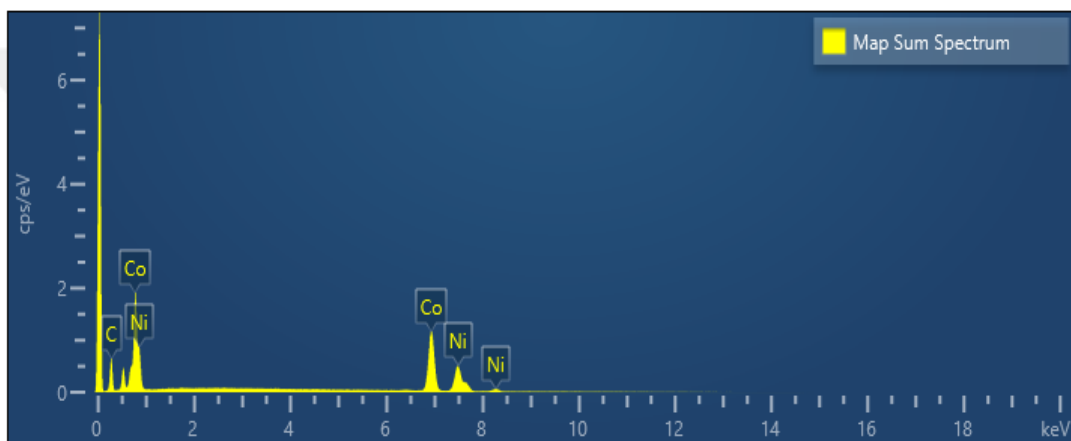
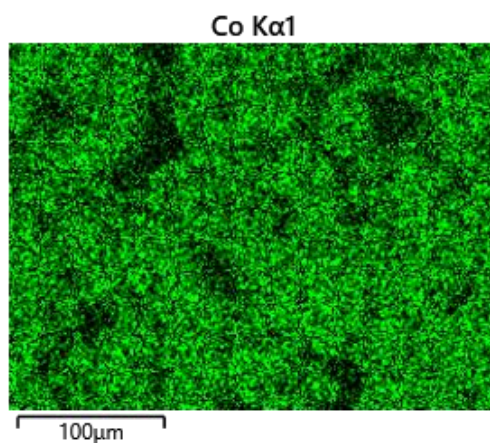
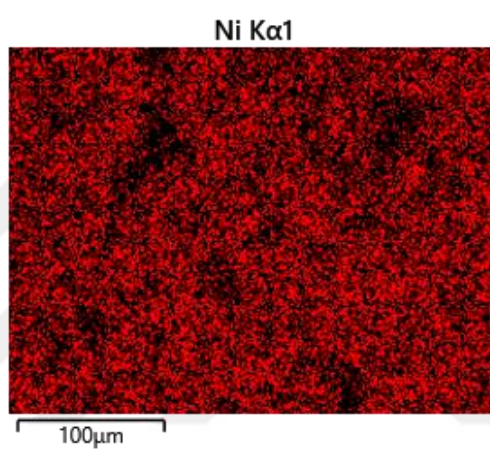


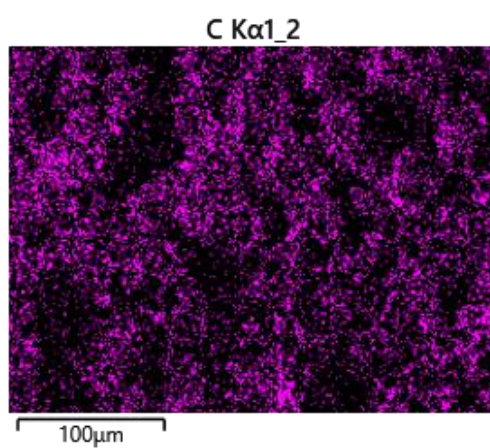
Figure 3.5 EDS Map Sum Spectrum of Ni-Co-Graphene coating (for Ramp current).



a)



b)



c)

Figure 3.6 EDS dot map analysis of Ni-Co-Graphene coatings produced by ramp current: a) copper, b) nickel, c) carbon.

3.1.3 X-Ray diffraction analysis

Ni-Co alloys and Ni-Co-Graphene coatings were examined by means of XRD. Wavelength of X-ray beam is selected as 1.54059 Å in XRD analysis. Card number of JPDS used in the analysis is 00-004-0850 [23]. XRD graphics are given below in Figure 3.7 and Figure 3.8. According to these results, peaks generally occur at (111), (200), (220) and (311) planes.

In DC current type, (200) plane is not observed and the highest intensity is obtained in (220) plane. Intensities of planes (111) and (311) are low and close to each other. In PC current type, (200) planes occur and it can be observed that intensities of (111) and (311) planes increase. For PRC, peak intensities change considerably. While intensities of (111) and (200) planes increase dramatically, intensity of (220) decreases significantly. For ramp current type, intensities of (111) and (200) planes decrease considerably and intensity of (220) planes increases. Intensity of (311) planes doesn't change that much.

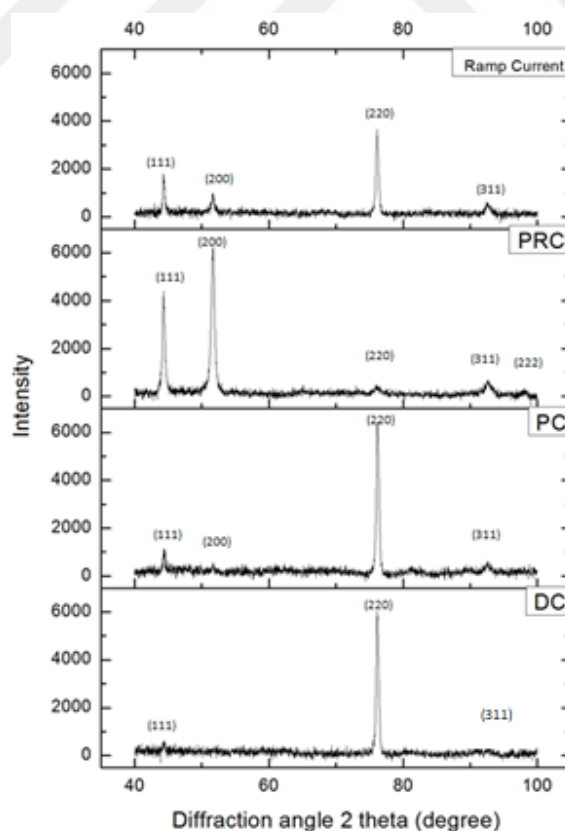


Figure 3.7 XRD patterns of Ni-Co alloy deposits.

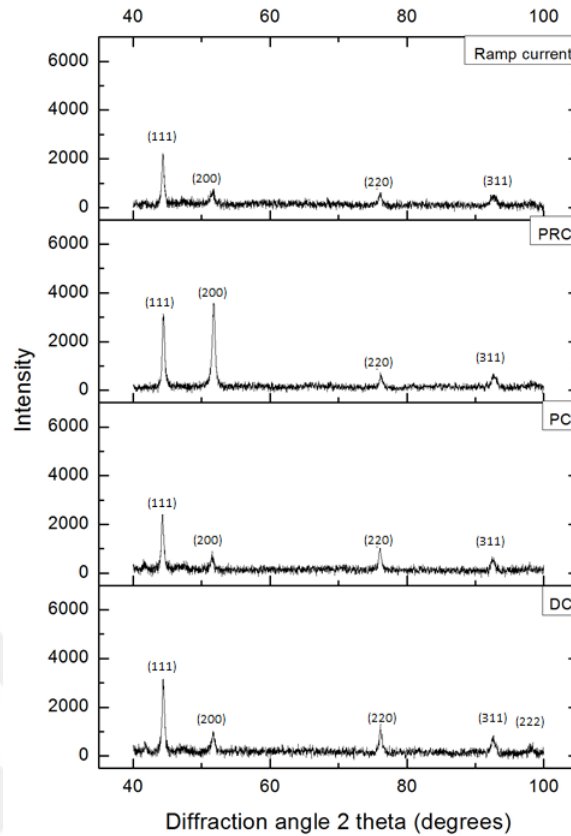


Figure 3.8 XRD patterns of Ni-Co-Graphene nanocomposite deposits.

When metal matrix nanocomposites are examined, intensities are observed to decrease. Addition of graphene decreases the intensities of all peaks. In DC types, (111) plane intensity of nanocomposite is higher than that of alloy. (200), (220), (311) and (222) planes are observed but their intensities are very low. (222) peak is only observed in DC type method. The intensity values for PC type are similar to those for DC type. While intensity of (200) plane increases, the other intensities don't change much. Grain growth in [111] direction is higher than other directions in ramp current. The other planes have low intensity and their intensity values are close to each other. The smaller the grain size is, the lower the intensity will be. When graphene reinforced material is added into coating, grain growth is inhibited and smaller grain size occurs due to the fact that graphene increases the nucleation and inhibits grain growth [3].

Crystal size affects properties of coatings. Crystal size was measured by Halder-Wagner method using PDXL program. In Figure 3.9, crystallite sizes of coatings are

given. Crystal sizes of planes validate the XRD results. Intensities of nanocomposite coatings are lower than those of alloy coatings.

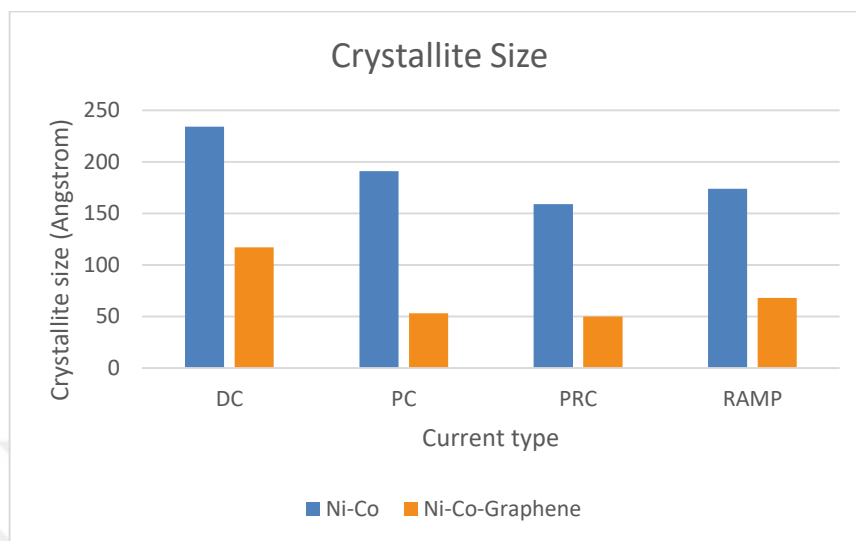


Figure 3.9 Crystallite sizes measured by Halder-Wagner method.

3.1.4 Hardness of coatings

According to many studies in literature, addition of second phase into alloys increases the hardness. It is thought that second phase locates on the grain boundary and decreases dislocation. Besides that, second phase increases the nucleation rate and decreases the finer grain size [58]. Hardness of produced alloys and composites were measured by Vickers microhardness test. The hardness results are given in Figure 3.10.

According to Vickers microhardness test values, current type has an effect on hardness values. The highest hardness value is obtained for Ni-Co-Graphene nanocomposites produced by PRC method. When comparing the hardness values according to current type, DC yields the lowest hardness value. If the current type is changed, hardness values will also be changed. The highest hardness value for Ni-Co alloys belongs to ramp current and it decreases with PRC, PC and DC types, respectively. On the other hand, the highest hardness value for Ni-Co-Graphene nanocomposites belongs to PRC method and then it decreases with ramp current, PC and DC type, respectively.

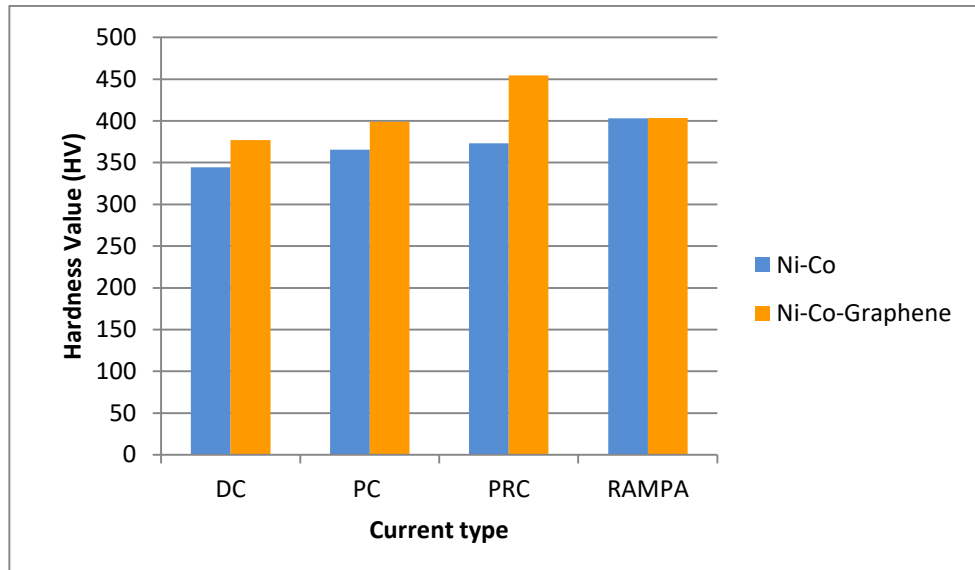


Figure 3.10 Hardness values for deposits with respect to current types and contents measured by Vickers microhardness test.

Chang et al. [35] reported that properties of Ni-Co-Al₂O₃ composites are superior to those of Ni-Co alloys. Composites have higher hardness value and wear resistance than alloys. They examined the current effects on the hardness. PRC current type provides better hardness than DC current type. They thought PRC method provides fine grain size, lower porosity and more compact structure.

Wang et al. [51] examined the effects of cobalt content on the Ni-Co alloys produced by electrodeposition. When cobalt content increases to some extent, hardness increases. Between 0% - 49%, cobalt increases the hardness but increasing cobalt further causes the hardness to decrease. The reason for this phenomenon is that cobalt rich alloys have higher grain size than nickel rich alloys.

Hu et al. [47] proved that current type affects deposition properties. For example, ramp current increases hardness. They declared that nucleation and grain growth is rivalry in electrodeposition process. In ramp current, sudden peak current gives rise to decomposition of crystal growth and new seeding occurs. Thus, finer grain size can be obtained by ramp current type. Grain size affects the microhardness, hence finer grain size provides higher hardness value.

Tao et al. [59] studied nano-sized copper coatings produced by electrodeposition. They also examined the effects of the current type. They compared direct current and

pulse current. They obtained that pulse current provides more homogenous surface, very fine grain and thus higher hardness values.

3.1.5 Thickness of coatings

Thickness of coatings were measured by coating thickness gauge. This gauge adopts magnetic method and eddy current method. The measurements were made by eddy current method. This method is used in non-conductive materials or non-ferrous materials [60]. Our coating materials are non-ferrous and we used eddy current method. The thickness results are given in Figure 3.11.

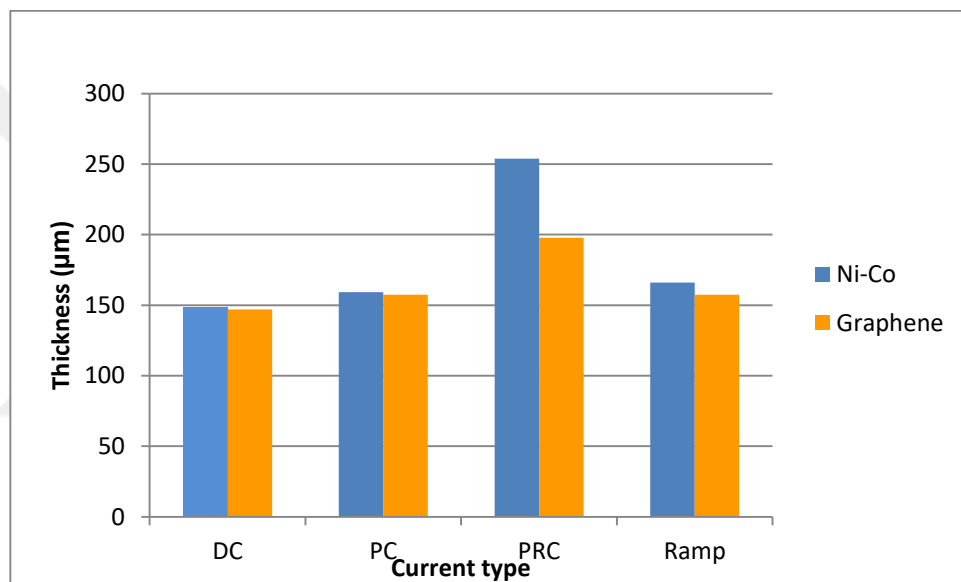


Figure 3.11 Thickness of Ni-Co and Ni-Co-Graphene coatings.

When examining the results, graphene reinforced coatings are thinner than Ni-Co alloys. The difference is the greatest when PRC type method is applied. Graphene reinforcement affects microstructure. Graphene acts as a physical barrier and inhibits grain growth, hence smaller grain size can be obtained. Smaller grain size may lead to thinner coatings [61].

When comparing the current types, the highest thickness value is obtained with PRC type and thickness decreases with ramp current, PC and DC type, respectively. The reason for that is the fact that maximum current value is 910 mA for PRC current type and higher current values cause to higher deposition rate and material.

3.2 Tribological properties

3.2.1 Wear and abrasion behavior

Wear tests were conducted by handmade wear machine and the results were obtained by computer program that belongs to this machine. Tests were conducted using 1 N loading, 500 m distance, speed of 25 mm/s, 12 mm trace width by reciprocating motion. As an abrasive material, steel ball of 10 mm diameter was used.

As a result of abrasion, wear trace occurred on the surface and tribological properties were examined using this trace and friction coefficient data. Wear trace width was taken by NIKON Eclipse MA100 inverted optical microscope with 50X magnification. Trace widths of Ni-Co alloys and Ni-Co-Graphene nanocomposites produced by DC, PC, PRC and ramp current types are given in Figure 3.12. Specimens were compared according to wear trace widths. Blue columns belong to Ni-Co alloys and when the wear trace of Ni-Co alloys are to be examined, it is seen that specimen produced by DC type has the highest trace width value. Besides that, trace width decreases for PC, PRC and ramp current, respectively. Therefore, current types affect grain growth mechanism and more compact and strong coatings are obtained towards the ramp current. Wear trace widths of materials produced by PC, PRC and ramp current types are close to each other.

Nanocomposites can be obtained by adding graphene reinforced materials into Ni-Co alloys. Their abrasion behavior is different from Ni-Co alloys. Examining the Figure 3.12, wear trace widths of composites are smaller than those of alloys. By current types, trace width decreases with the current types of DC, ramp, PC and PRC, respectively. It is compatible with EDS results. The lowest ratio of carbon content belongs to the specimen produced by DC type. Graphene provides lubricating, hence trace width is the highest for the specimen produced by DC. When alloys and composites are to be compared, wear trace widths of alloys are higher than those of composites. It is estimated that graphene acts as a physical barrier to grain growth and inhibits it, thus lower trace widths were obtained because of smaller grain size.

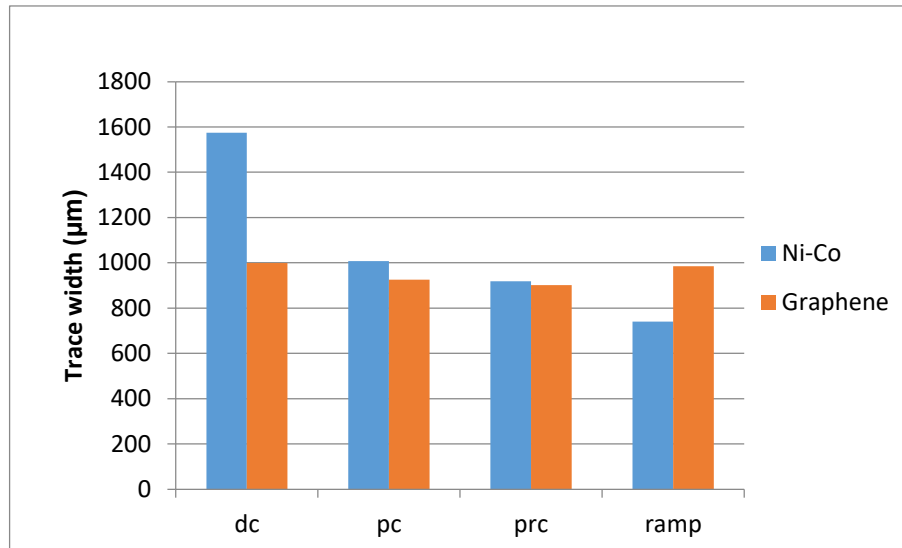


Figure 3.12 Results of wear trace width.

Friction coefficient values recorded during the wear tests are given in Figure 3.13 and friction coefficient as function of distance for the Ni–Co alloy and Ni–Co–Graphene nanocomposite deposits produced by pulse current are given Figure 3.14 and Figure 3.15. Examining the Figure 3.13, friction coefficients change by current type and addition of graphene. Comparing Ni-Co alloys and Ni-Co-Graphene composites, composites have lower friction coefficients than alloys because of the lubricating effect of graphene. It also has an effect on wear trace width. Xue et al. [62] reported that when comparing nickel coating with nickel graphene coating produced by pulse current, friction coefficient of nickel coating is higher than that of Ni-Graphene composite. They reported that graphene transforms to graphite during wearing process and it acts as a lubricate material.

Considering the effects of current types, similar results are reported by Su et al. [63]. In their study, they reported that specimens produced by DC method have smaller friction coefficient. The reason of this is thought that grain sizes of specimens produced by PC, PRC and ramp current types are smaller than that of DC type. Wang et al. [51] reported that cobalt rich alloys have smaller friction coefficient than nickel rich alloys. Results of EDS analysis show that DC type provides higher cobalt content.

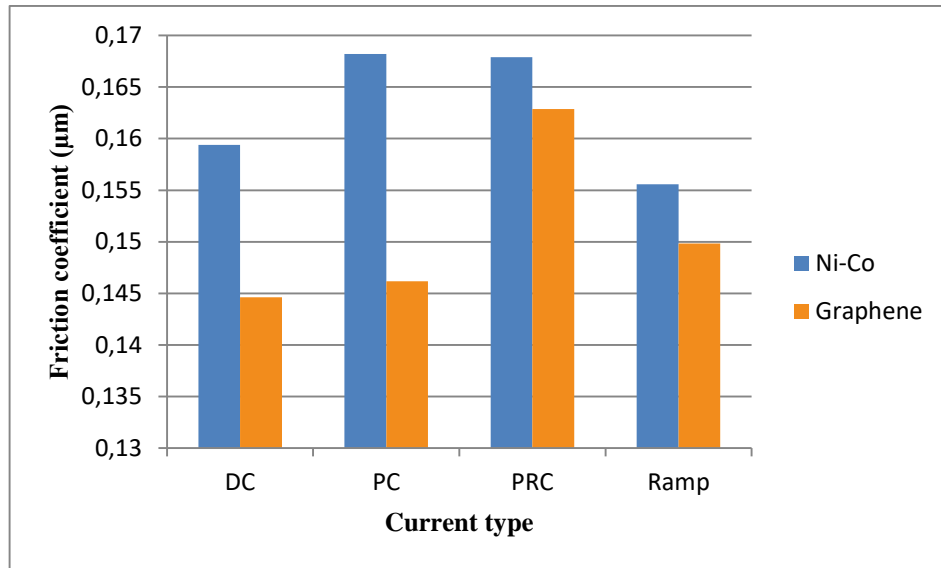


Figure 3.13 Friction coefficient as function of current type in the deposits.

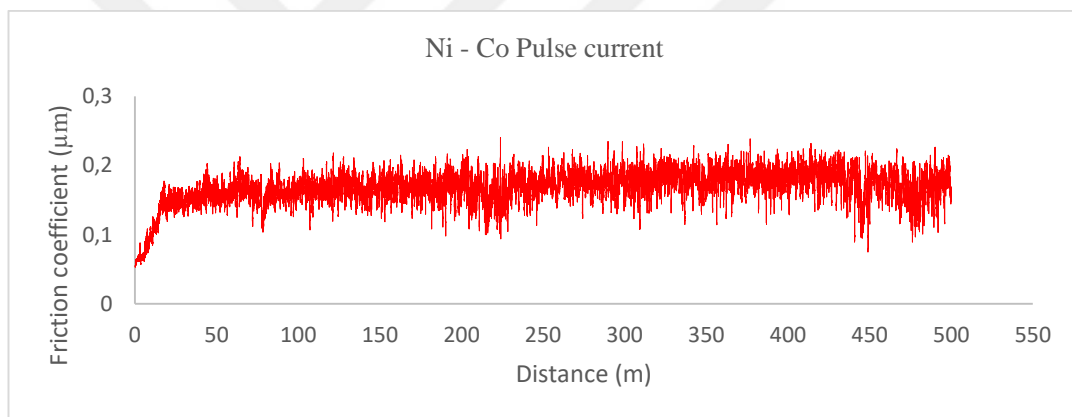


Figure 3.14 Friction coefficient as function of distance for the Ni–Co alloy deposits produced by pulse current.

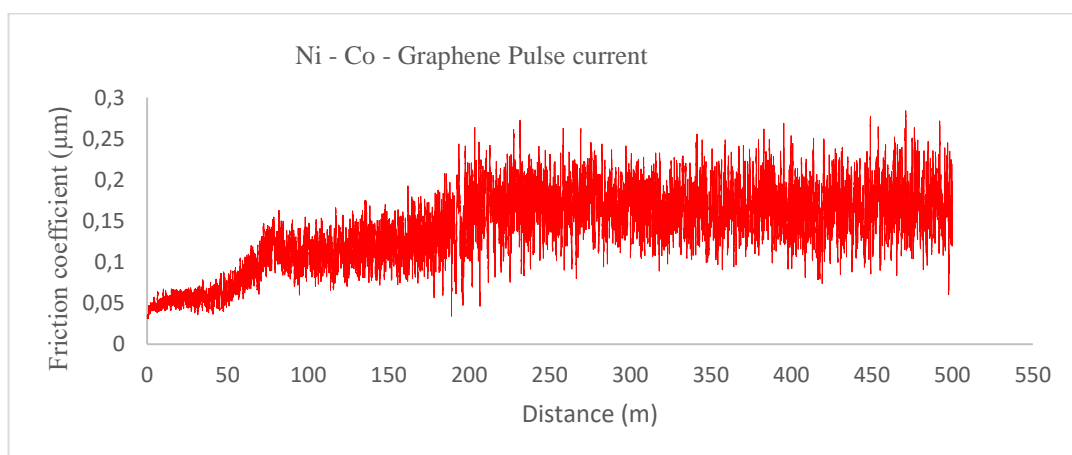


Figure 3.15 Friction coefficient as function of distance for the Ni–Co–Graphene alloy deposits produced by pulse current

Wear track images taken by optical microscope are given in Figure 3.16. Wear track widths were measured by using these images. When comparing alloys with composites, different abrasive mechanism is observed. Wear track widths of Ni-Co alloys are wider than those of composites.

The SEM images of worn surfaces of Ni-Co alloys and Ni-Co-Graphene nanocomposites are given in Figure 3.16. As examining Ni-Co images, microcracks can be observed due to plastic deformation. These microcracks cause delamination. Oxidation occurs by abrasion and oxide layer moves out of the surface due to their fatigue. Thus, abrasive track occurs on the surface. For Ni-Co alloys produced by DC type, SEM images and EDS results proof this case. As it can be seen from Figure 3.17, worn area has higher oxygen content because of more delamination occurred and iron on the surface comes from the abrasive ball.

As Ni-Co alloys are compared considering the current types, DC type has delamination mechanism. Some parts are removed from the surface by abrasive motion. For PC type, delamination parts are smaller than those for DC type and abrasive wear tracks are observable. PRC type generally has abrasive wear tracks and ramp current behaves like PC and PRC type. It is commented that these results are obtained because of their compact structure of PRC, PC and ramp current types and hardness results proof this case. Same results are observed for graphene reinforced composites with respect to current types. Surface of specimens produced by DC type has delamination area whereas delamination for PC type is not observed and abrasive wear occurs instead. The smoothest wear surface belongs to PRC type. As comparing Ni-Co alloys and graphene reinforced Ni-Co composites, graphene acts as a lubricating material and worn surface of it is better than the worn surface of Ni-Co alloys (see Figure 3.18).

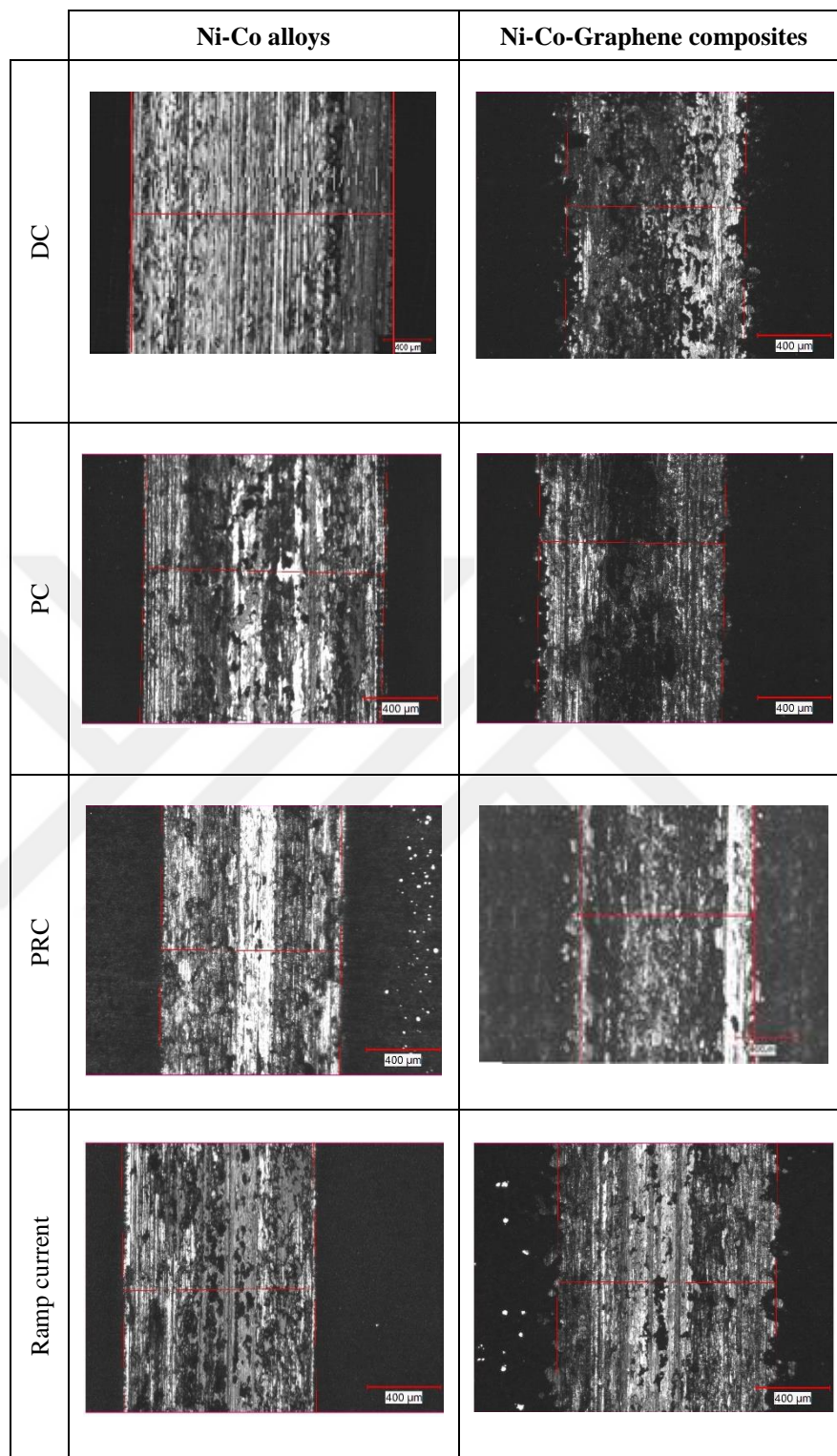


Figure 3.16 Wear track images of Ni-Co alloys and Ni-Co-Graphene composites.

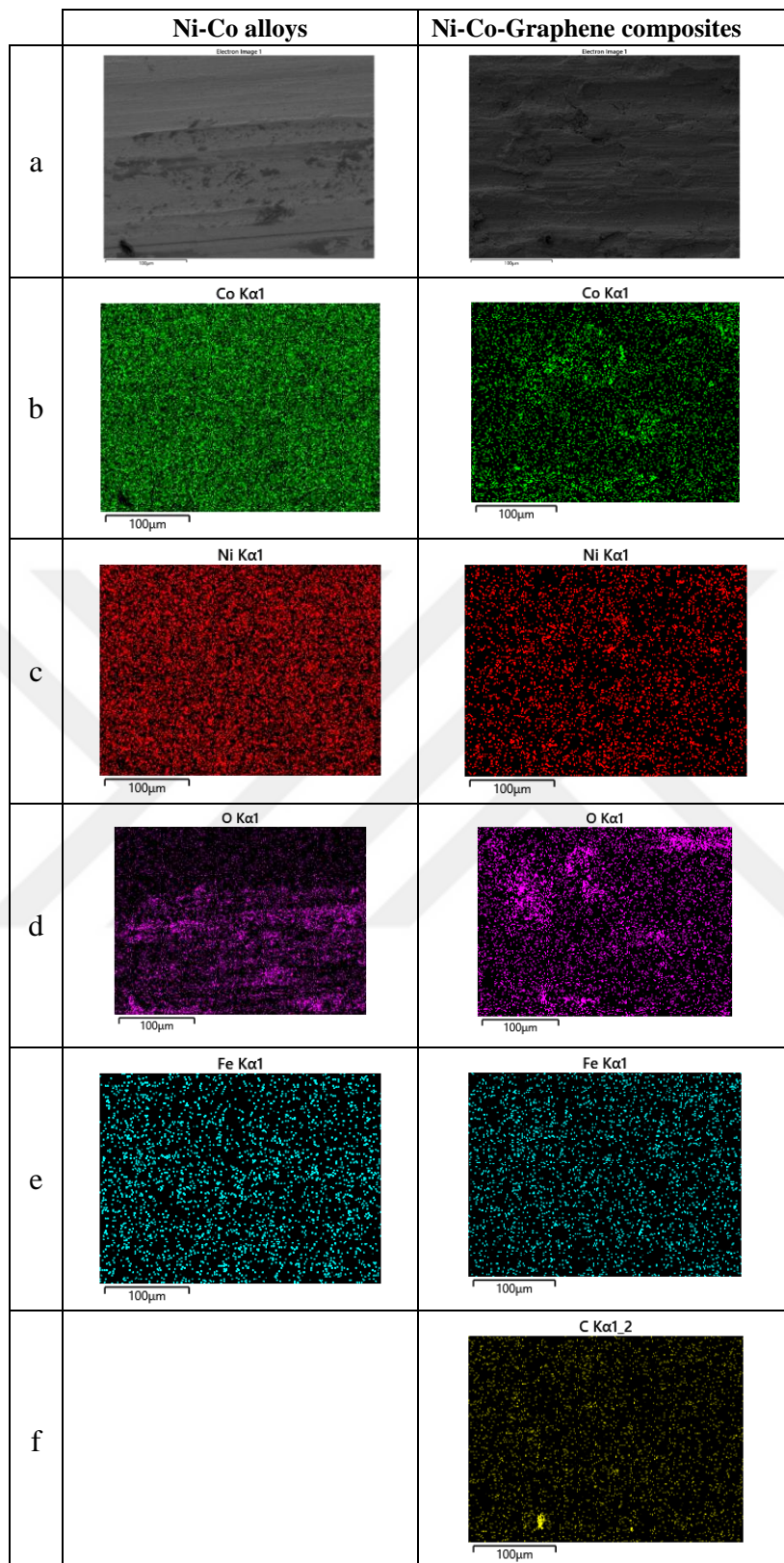


Figure 3.17 Ni-Co-Graphene coatings wear trace and EDS dot map analyzes of Ni-Co alloys produced by DC current: a) SEM images, b) map of cobalt, c) map of nickel, d) map of oxygen, e) map of iron, f) map of carbon.

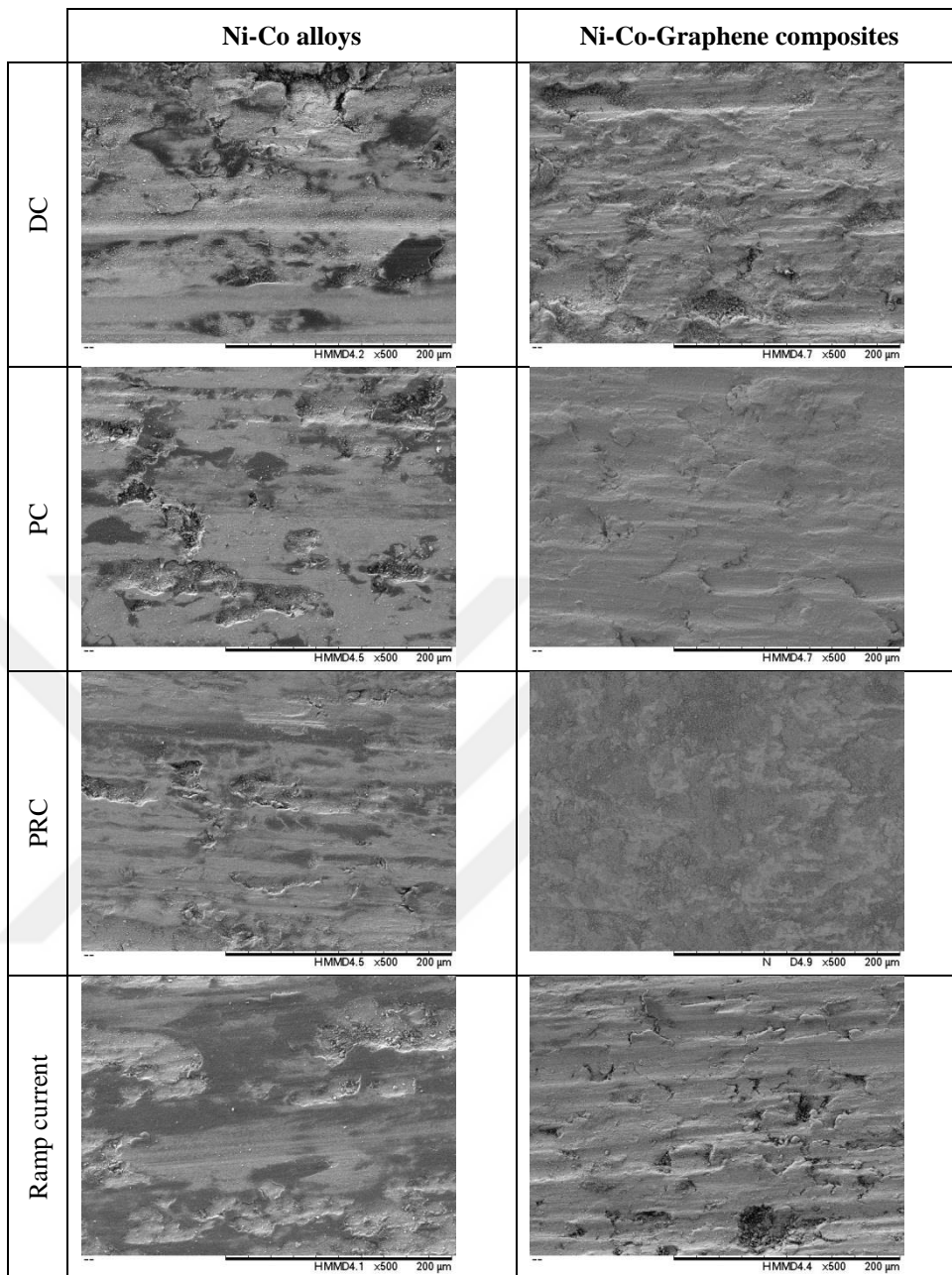


Figure 3.18 SEM surface image of wear trace of Ni-Co alloys and Ni-Co-Graphene coatings according to current types.

CHAPTER 4

CONCLUSION AND FUTURE WORK

In this study, Ni-Co alloy and Ni-Co-Graphene metal matrix nanocomposite coatings were produced by electrodeposition method by applying different current types which are direct current, pulse current, pulse-reverse current and ramp current. Copper was used as a substrate. Effects of graphene addition and current type on microstructural, mechanical and tribological properties of deposition were examined.

Phase analysis, elemental analysis, microstructural examination, analysis of mechanical properties and the investigation of tribological properties were performed to illustrate the effects of current types and graphene addition in Ni-Co alloys.

It was observed that grain size changed by current type. For Ni-Co alloys, grain size decreases for DC, PC, ramp current and PRC type, respectively. Similarly, this case is exactly valid for Ni-Co-Graphene metal matrix nanocomposites. As comparing alloys and composites, composites have smaller grain size due to the fact that graphene inhibits the grain growth.

EDS analysis gives the elemental ratio values. Graphene content changes by current type. The highest graphene ratio belongs to ramp current and it decreases with PRC, PC, and DC types, respectively. Cobalt ratio also changes by current type. Similar to graphene, the highest cobalt content belongs to DC type and decreases with PC, ramp and PRC types, respectively.

According to XRD results, planes are mostly occurred at (111), (200), (220), (311) values for Ni-Co alloys. For (111) and (200) planes, intensity values for DC type are the smallest and they increase for PC, ramp current and PRC type, respectively. For graphene reinforced composites, grain growth occurs in [111], [200], [220], [311] directions. Directions of grain growth don't change by reinforcement material but their intensities decrease because graphene decreases the grain size.

Hardnesses are affected by current type. The highest hardness value belongs to PRC type and decreases with ramp current, PC and DC types, respectively. Hardnesses of Ni-Co-Graphene metal matrix nanocomposites are higher than those of Ni-Co alloys.

Coating thicknesses of alloys and composites are close to each other. Thicknesses of composite coatings are higher than those of alloys. Thickness of coatings produced by PRC type is the highest and those produced by ramp current, PC and DC type decreases, respectively.

Moreover, friction coefficient changes by current types and addition of graphene. DC type causes to lower friction coefficient due to high cobalt content. The smallest cobalt content and the highest friction coefficient belongs to PRC type. Graphene reinforced metal matrix nanocomposites have lower friction coefficient than Ni-Co alloys.

Wear track widths of Ni-Co alloys are higher than those of graphene reinforced composites except for the ramp current type. widths of alloy specimens produced by DC type have the highest values and widths of other specimens produced by PC, PRC and ramp current types have lower values, respectively. On the other hand, considering composite coatings, widths of the specimens produced by DC and ramp current are close to each other and higher than those produced by PC and PRC types.

PRC type causes smaller worn surface since it has more compact structure. For composites, graphene acts as a lubricating material.

REFERENCES

- [1] “Technical Data for the Element Nickel in The Periodic Table.” [Online]. Available: “<http://www.periodictable.com/Elements/028/data.html> ” [Accessed: 04.07.2017].
- [2] Tian,L. & Xu, J. & Qiang, C. “The Electrodeposition Behaviors and Magnetic Properties of Ni-Co Films” *Appl. Surf. Sci.*, 257(10), 4689-4694, 2011.
- [3] Shi, L. & Sun, C. F. & Gao, P. & Zhou, F. & Liu, W. M. “Electrodeposition and Characterization of Ni-Co-Carbon Nanotubes Composite Coatings,” *Surf. Coat. Technol.*, 200(16), 4870–4875, 2006.
- [4] Osaka, T. “Electrodeposition of Highly Functional Thin Films for Magnetic Recording Devices of the Next Century,” *Electrochimica Acta*, 45(20), 3311-3321, 2000.
- [5] Kandpal, B. C. & Kumar, K. & Kandpal, H. S. “Production Technologies of Metal Matrix Composite: A Review,” *IJRMET*, 4, 27-32, 2014.
- [6] Xavior, M. A. & Kumar, H. “Processing and Characterization Techniques of Graphene Reinforced Metal Matrix Composites (GRMMC); A Review,” *Mater. Today Proc.*, 4(2), Part A, 3334–3341, 2017.
- [7] Liu, C. & Su, F. & Liang, J. “Producing Cobalt–Graphene Composite Coating by Pulse Electrodeposition with Excellent Wear and Corrosion Resistance,” *Appl. Surf. Sci.*, 351, 889–896, 2015.
- [8] ASM International Handbook Committee, “ASM Specialty Handbook, Nickel, Cobalt, and Their Alloys” , ASM International, Ohio, 2000.
- [9] Maden Mühendisleri Odası, “TMMOB Maden Mühendisleri Odası Nikel Raporu ”, Gurup Matbaacılık, ANKARA, 2012.

- [10] Pedersen, T. & ET, L. S. C. “Facts About Nickel,” [Online]. Available: “<https://www.livescience.com/29327-nickel.html>.” [Accessed: 21.07.2017].
- [11] “Cobalt and Cobalt Alloys.” [Online]. Available: <http://www.totalmateria.com/Article54.htm>., [Accessed: 04.07.2017].
- [12] “Cobalt Research” [Online]. Available: “<http://www.bhpl.biz/projects/cobalt-deposits/cobalt-research/>”, [Accessed: 04.07. 2017].
- [13] ASM International Handbook Committee, “Copper and Copper Alloys. ASM International”, ASM International, Ohio,2001.
- [14] H. W. Richardson, “Handbook of Copper Compounds and Applications.” CRC Press, Mishawaka,1997.
- [15] Pati, S. K. & Enoki, T. & Rao, C. N. R., “Graphene and Its Fascinating Attributes”, World Scientific, Singapore, 2011.
- [16] T. M. Group, “Complex Multifunctional Polymer/Carbon-Nanotube Composites - Nasa Tech Briefs: Tech Briefs” [Online]. Available: “<http://www.techbriefs.com/component/content/article/ntb/tech-briefs/materials/3540>.” [Accessed: 22.07.2017].
- [17] “Bonding (Inter/Intra),” Graphene [Online]. Available: “<http://grapheene.weebly.com/bonding-interintra.html>.”,[Accessed: 4.07.2017].
- [18] Sharon, M. & Sharon, M. “Graphene: An Introduction to the Fundamentals and Industrial Applications”, John Wiley & Sons, Beverly, 2015.
- [19] Ray, S. “Applications of Graphene and Graphene-Oxide Based Nanomaterials”, William Andrew, Waltham, 2015.
- [20] Warner, J. H. & Schaffel, F. & M. Rummeli, & Bachmatiuk, A., “Graphene: Fundamentals and Emergent Applications”, Newnes, Waltham, 2013.
- [21] Chung, D. D. L. “Composite Materials: Science and Applications”, (2nd edition) Springer Science & Business Media, 2010, USA.

- [22] Y. Nishida, "Introduction to Metal Matrix Composites: Fabrication and Recycling", Springer Science & Business Media, New York, 2013.
- [23] Karslıoğlu, R. "Karbon Nanotüp Takviyeli Nikel-Kobalt Kaplamaların Geliştirilmesi", M. Sc. Thesis, Sakarya University, Graduate School of Natural and Applied Sciences, Sakarya-Turkey, 2014.
- [24] Cha, K. K., "Composite Materials: Science and Engineering", (2nd edition) Springer Science & Business Media, USA, 2013.
- [25] Cha, S. I. & Kim, K. T. & Lee, K. H. & Mo, C. B. & Hong, S. H. "Strengthening and Toughening of Carbon Nanotube Reinforced Alumina Nanocomposite Fabricated by Molecular Level Mixing Process" *Scr. Mater.*, 53(7), 793-797, 2005.
- [26] Ceschini, L. & Dahle, A. & Gupta, M. & Jarfors, A. E. & Jayalakshmi, S. Morri, A. & Rotundo, F. & Toschi, S. & Singh, R. A. "Aluminum and Magnesium Metal Matrix Nanocomposites", (1st edition), Springer, Singapore 2017.
- [27] Ajayan, P.M. & Schadler, L.S. & Braun, P.V. "Nanocomposite Science and Technology", John Wiley & Sons, Germany, 2006.
- [28] Twardowski, T. E., "Introduction to Nanocomposite Materials: Properties, Processing, Characterization", DEStech Publications, Pennsylvania, 2007.
- [29] Dini, J. W. "Electrodeposition: The Materials Science of Coatings and Substrates", Noyes Publications, USA, 1993.
- [30] Mallory, G. O. & Hajdu, J. B. "Electroless Plating: Fundamentals and Applications", Cambridge University Press, Newyork, 1990.
- [31] Zhang, B. "Amorphous and Nano Alloys Electroless Depositions: Technology, Composition, Structure and Theory", Elsevier, USA, 2015.

- [32] “Electroless Plating Method, Electroless Plating Techniques, SPC.” [Online]. Available: <http://www.sharrettsplating.com/plating-methods/electroless-plating>. [Accessed: 02.07.2017].
- [33] “Copper Electroplating Fundamentals, Dow Electronic Materials.” [Online]. Available: <http://blog.dowelectronicmaterials.com/en/posts/2016/11/copper-electroplating-fundamentals>. [Accessed: 07.07.2017].
- [34] Gamburg, Y. D. & Zangari, G. “Theory and Practice of Metal Electrodeposition”, Springer Science & Business Media, USA, 2011.
- [35] Chang, L. M. & An, M. Z. & Shi, S. Y. “Microstructure and Characterization of Ni-Co/Al₂O₃ Composite Coatings by Pulse Reversal Electrodeposit,” Mater. Chem. Phys., 100(2), 395–399, 2006.
- [36] Hu, F. & Chan, K. C. “Electrocodeposition Behavior of Ni–SiC Composite Under Different Shaped Waveforms,” Appl. Surf. Sci., 233(1), 163-171, 2004.
- [37] Chandrasekar, M. S. & Pushpavanam, M. “Pulse and Pulse Reverse Plating- Conceptual, Advantages and Applications,” Electrochimica Acta, 53(8), 3313-3322, 2008.
- [38] Landolt, D. & Marlot, A. “Microstructure and Composition of Pulse-Plated Metals and Alloys,” Surf. Coat. Technol., 169, 8–13, 2003.
- [39] Harrigan, W. C. “Commercial Processing of Metal Matrix Composites,” Mater. Sci. Eng. A, 244(1), 75–79, 1998.
- [40] Angelo, P. C. & Subramanian, R. “Powder Metallurgy: Science, Technology And Applications ”, PHI Learning Pvt. Ltd., New Delhi, 2008.
- [41] Heimann, R. B. “ Plasma-Spray Coating: Principles and Applications”, John Wiley & Sons, USA, 2008.

- [42] “Plasma Spraying - Ceramic Spraying - Zirconium Sprayers - Yttrium Sprayers - Chrome Sprayers - Tungsten Sprayers.” [Online]. Available: <http://www.amphardchrome.co.uk/plasma-spraying.php>. [Accessed: 7.06.2017].
- [43] Kim, J. S. & Kwon, Y. S. & Lomovsky, O. I. & Dudina, D.V. & Kosarev, V. F. & Klinkov, S. V. & Kwon, D. H. & Smurov, I. “Cold Spraying of in situ Produced TiB₂-Cu Nanocomposite Powders,” *Compos. Sci. Technol.*, 67(11), 2292–2296, 2007.
- [44] Sudharshan, P. & Vishnukanthan, V. & Sundararajan, G. “Effect of Heat Treatment on Properties of Cold Sprayed Nanocrystalline Copper Alumina Coatings,” *Acta Mater.*, 55(14), 4741–4751, 2007.
- [45] “MEC, Cold Spray, Metallizing Equipment Co. Pvt. Ltd.” [Online]. Available: <http://www.mecpl.com/cold-spray.php>. [Accessed: 07.07.2017].
- [46] Karşlıoğlu R. & Akbulut, H. “Comparison Microstructure and Sliding Wear Properties of Nickel-Cobalt/CNT Composite Coatings by DC, PC and PRC Current Electrodeposition,” *Appl. Surf. Sci.*, 353, 615–627, 2015.
- [47] Hu, F. & Chan, K. C. “Equivalent Circuit Modelling of Ni-SiC Electrodeposition under Ramp-up and Ramp-down Waveforms,” *Mater. Chem. Phys.*, 99(2), 424–430, 2006.
- [48] Srivastava, M. & Selvi, V. & Grips, V. K. & Rajam, K. S. “Corrosion Resistance and Microstructure of Electrodeposited Nickel-Cobalt Alloy Coatings,” *Surf. Coat. Technol.*, 201(6), 3051–3060, 2006.
- [49] D. Shechter, “Ultrasonic Homogenizers vs. High Pressure Homogenizers.” [Online]. Available: <http://www.beei.com/blog/ultrasonic-homogenizers-vs-high-pressure-homogenizers>. [Accessed: 15.06.2017].
- [50] “Tabletop Microscope TM3030Plus: Hitachi High-Technologies in Europe.” [Online]. Available: http://www.hitachi-igtech.com/eu/product_detail/?pn=em-tm3030plus&version=. [Accessed: 15-Jul-2017].

- [51] Wang, . & Gao, Y. & Xue, Q. & Liu, H. & Xu, T. "Microstructure and Tribological Properties of Electrodeposited Ni-Co Alloy Deposits", *Appl. Surf. Sci.*, 242(3-4), 326-332, 2005.
- [52] Shi, L. & Sun, C. & Liu, W. "Electrodeposited Nickel-Cobalt Composite Coating Containing MoS₂", *Appl. Surf. Sci.*, 254(21), 6880-6885, 2008.
- [53] Shi, L. & Sun, C. F. & Zhou, F. & Liu, W. M. "Electrodeposited Nickel-Cobalt Composite Coating Containing Nano-sized Si₃N₄", *Mater. Sci. Eng. A*, 397(1), 190-194, 2005.
- [54] Golodnitsky, D. & Rosenberg, Y. & Ulus, A. "The Role of Anion Additives in the Electrodeposition of Nickel-Cobalt Alloys from Sulfamate Electrolyte," *Electrochimica Acta*, 47(17), 2707-2714, 2002.
- [55] Steinbach, J. & Ferkel, H. "Nanostructured Ni-Al₂O₃ Films Prepared by DC and Pulsed DC Electroplating," *Scr. Mater.*, 44(8-9), 1813-1816, 2001.
- [56] Ranjith, B. & Kalaignan, P. G. "Ni-Co-TiO₂ Nanocomposite Coating Prepared by Pulse and Pulse Reversal Methods Using Acetate Bath," *Appl. Surf. Sci.*, 257(1), 42-47, 2010.
- [57] Schweckandt, D. S. & Aguirre, M. del C. "Electrodeposition of Ni-Co Alloys. Determination of Properties to be Used as Coins," *Procedia Mater. Sci.*, 8, 91-100, 2015.
- [58] Bakhit, B. & Akbari, A. "Effect of Particle Size and Co-deposition Technique on Hardness and Corrosion Properties of Ni-Co/SiC Composite Coatings," *Surf. Coat. Technol.*, 206(23), 4964-4975, 2012.
- [59] Tao, S. & Li, D. Y. "Tribological, Mechanical and Electrochemical Properties of Nanocrystalline Copper Deposits Produced by Pulse Electrodeposition," *Nanotechnology*, 17(1), 65, 2006.

- [60] “What is a Coating Thickness Gauge?” [Online]. Available: <http://www.elcometer.com/en/coating-thickness-gauge.html>. [Accessed: 20.07.2017].
- [61] Borkar, T. “Electrodeposition of Nickel Composite coatings,” M.Sc. Thesis, Mumbai, Maharashtra, INDIA, 2007.
- [62] Xue, Z. & Lei, W. & Wang, Y. & Qian, H. & Li, Q. “Effect of Pulse Duty Cycle on Mechanical Properties and Microstructure of Nickel-Graphene Composite Coating Produced by Pulse Electrodeposition under Supercritical Carbondioxide,” *Surf. Coat. Technol.*, 325, 417–428, 2017.
- [63] Su, F. & Liu, C. & Huang, P. “Establishing Relationships between Electrodeposition Techniques, Microstructure and Properties of Nanocrystalline Co-W Alloy Coatings”, *J. Alloys Compd.*, 557, 228–238, 2013.

CURRICULUM VITAE

PERSONAL INFORMATION

Name Surname : Aynur İNAN ÜSTÜN
Date of Birth : 1988
E-mail : ainan@ybu.edu.tr



EDUCATION

High School : Kazım Ayan Anatolian High School / SİVAS
Bachelor : Erciyes University / KAYSERİ
Master Degree : Ankara Yıldırım Beyazıt University

WORK EXPERIENCE

Research Assist. : Ankara Yıldırım Beyazıt University / (2014-continued)

